FISEVIER

Contents lists available at ScienceDirect

Palaeogeography, Palaeoclimatology, Palaeoecology

journal homepage: www.elsevier.com/locate/palaeo



Ichnofabrics and chemostratigraphy argue against persistent anoxia during the Upper Kellwasser Event in New York State



Emily E. Haddad^{a,*}, Diana L. Boyer^b, Mary L. Droser^a, Bridget K. Lee^a, Timothy W. Lyons^a, Gordon D. Love^a

ARTICLE INFO

Keywords: Devonian Trace fossils Iron speciation Trace metals Molybdenum Lipid biomarkers

ABSTRACT

Organic-rich strata coeval with bioevents of varying magnitudes characterize global Devonian sedimentary successions. The Upper Kellwasser (UKw) black shale depositional event is coincident with the largest pulse of diversity loss within the marine Late Devonian mass extinction and has been shown to be an ecologically critical turnover for shallow-water species. Marine anoxia/euxinia is widely thought to be an important and ubiquitous driver of this biotic crisis, though the duration, intensity, and global extent of these environmental conditions during the UKw event are not well-constrained.

We characterized redox conditions during deposition of the UKw in the northern Appalachian Basin to constrain local variability and relative magnitude of dissolved oxygen fluctuations. We used a combination of proxies relating to the bottom waters, water column, and photic zone to compile an integrated picture of basinal oxygen dynamics. Our multi-faceted approach combines trace fossil evidence for faunal activity at the sediment-water interface with inorganic and organic geochemical proxies for redox conditions within the water column. Minor biological disruptions to laminated sedimentary fabric indicate at least intermittent oxygenation of the bottom waters during deposition of the UKw, albeit in a low dissolved oxygen seafloor setting. Trace metal proxies (Mo, Mn, U and V) and Fe mineral speciation provide compelling evidence for a water column experiencing intermittent rather than persistent anoxic/euxinic conditions. Lipid biomarkers reinforce the interpretation of variable dissolved oxygen conditions with very low concentrations of Chlorobi carotenoid biomarkers pointing to seasonal/rare episodes of photic zone euxinia. This integrated dataset provides evidence for local redox variability in UKw deposition and supports the likelihood that marine anoxia and euxinia were not globally persistent at the Frasnian-Famennian boundary.

1. Introduction

There are numerous organic-rich deposits in global Devonian strata associated with biotic turnover events of varying magnitude (House, 2002). The diversity crisis at the Frasnian-Famennian (F/F) stage boundary (376 Ma), correlative with the Upper Kellwasser (UKw) depositional event, has long been characterized as one of the "Big 5" Phanerozoic Mass Extinctions (Raup and Sepkoski, 1982; Jablonski, 1991; McGhee, 1996). Paleontological studies of diversity trends for marine invertebrates have recognized a protracted and unexplained drop in diversity from the Givetian (middle-Devonian) through the Famennian (end-Devonian) linked to suppressed origination rates and peaks in extinction, most appropriately termed biodiversity crises, at the end-Givetian, end-Frasnian, and end-Famennian stage boundaries (Bambach et al., 2004; Bambach, 2006; Alroy, 2008a, 2008b; Stigall,

2011). Though the significance of the Late Devonian bioevents as mass extinctions has been deemphasized based on traditional criteria for magnitude and duration (Foote, 1994; Bambach et al., 2004; Alroy, 2008b), marine invertebrate community restructuring resulting from these periods of enhanced extinction rates must have been ecologically critical (Droser et al., 2000; McGhee et al., 2004) and constituted a turning point at the end-Devonian in the evolutionary history of reef communities, vertebrates, and primary producers (Fagerstrom, 1994; Sallan and Coates, 2010; Schwark and Empt, 2006).

Despite their evolutionary importance, the mechanisms and associated environmental conditions that drove Late Devonian biocrises remain enigmatic. Marine anoxia and/or euxinia are widely thought to be important contributing factors to these turnover events, in part because of the pervasiveness of black shale preservation coeval with declining diversity (Joachimski and Buggisch, 1993; Becker and House,

E-mail address: emily.haddad@email.ucr.edu (E.E. Haddad).

^a Department of Earth Sciences, University of California, Riverside, Riverside, CA 92521, USA

^b Department of Chemistry, Physics, & Geology, Winthrop University, Rock Hill, SC 29733, USA

^{*} Corresponding author.

1994; Joachimski et al., 2001; Levman and Von Bitter, 2002; Bond et al., 2004; Brown and Kenig, 2004; Tribovillard et al., 2004; Bond and Wignall, 2008; Carmichael et al., 2014). However, the persistence and geographical extent of marine anoxia during each black shale/bituminous limestone depositional event are often not well constrained, and it remains unresolved whether anoxia, or more specifically euxinia (toxic hydrogen sulfide accumulating in the water column), can be reasonably evoked as a geographically widespread primary kill mechanism.

We present a dataset of broadly applied but rarely combined proxies to characterize the oxygen dynamics of the water column during the UKw depositional event at the F/F boundary to better understand the event's potential impact on marine life and extinction. While the black shales of the Devonian Appalachian Basin have long been cited as classic examples of Black Sea-type stagnant, persistently euxinic basin deposits (Byers, 1977; Ettensohn, 1992), it is increasingly recognized that the organic-rich facies capture a range of bottom water redox conditions and do not represent homogenous depositional regimes. Importantly, previous studies of Appalachian Basin deposits have strongly suggested that not all the Devonian black shales were deposited in a pervasively euxinic basin (Murphy et al., 2000a, 2000b; Werne et al., 2002; Sageman et al., 2003; Boyer and Droser, 2011; Boyer et al., 2011).

Frequently cited systemic mechanisms for widespread anoxia (i.e., eustatic transgression, eutrophication, warming events, oceanic turnover, and/or stagnation) imply additional effects, including habitat loss, temperature and nutrient stress, and ecosystem collapse, which may serve as drivers of extinction (Berry and Wilde, 1978; Wilde and Berry, 1984, 1986; Johnson et al., 1985; Hallam, 1989; Becker, 1993; Joachimski and Buggisch, 1993; Algeo et al., 1995; Murphy et al., 2000b). Determining the significance of anoxia in the Late Devonian in binary terms of 'presence or absence' fails to capture complex Earth-life systems dynamics. While anoxia as a primary mechanism of global extinction must be shown to be both globally synchronous and widespread, the severity of anoxia, as determined by both spatial extent (vertically through the water column and laterally across the basin) and duration, must also be investigated on a global scale. Here we contribute a piece to the more complicated puzzle: an integrated ichnological and geochemical dataset from an UKw-equivalent black shale in the Appalachian Basin of New York, USA, in an attempt to shed light on the extent, stability, and duration of anoxia at the F/F boundary in this Laurentian basin. Our assertion is that global mechanisms will only become clear when viewed through the lens of numerous, comprehensive local studies. Our contribution to this goal employs a novel microstratigraphic sampling strategy that has the potential to capture small-scale variations in both biological and geochemical parameters.

2. Materials and methods

We examined continuous sedimentary sequences through the UKw black shale bed at four localities across a 60 km transect in western New York State (USA). These are, from most distal to most shoreward, Walnut Creek (WC), Eighteenmile Creek (EMC), Irish Gulf (IG), and Beaver Meadow Creek (BMC) (Fig. 1). The UKw Event is expressed in the Appalachian Basin as the Point Gratiot Bed (PGB), a black shale unit in the Hanover Formation of the Java Group (Over et al., 2013); this black shale bed ranges from 19 cm thick at Walnut Creek to almost 70 cm thick at Beaver Meadow Creek (Fig. 2). The F/F boundary has been well-constrained at these localities via conodont biostratigraphy (Over, 1997, 2002). The Hanover Formation consists of light gray or green, silty shale interbedded with dark gray or black, organic-rich silty shale and is underlain by the black Pipe Creek Shale Member (interpreted to preserve the Lower Kellwasser event; Over, 1997) and overlain by the petroliferous Dunkirk Shale.

Samples were collected from freshly exposed stream cuts and excavated outcrop in duplicate for biomarker, ichnofabric, and inorganic geochemical analysis; unweathered inner rock portions were used for

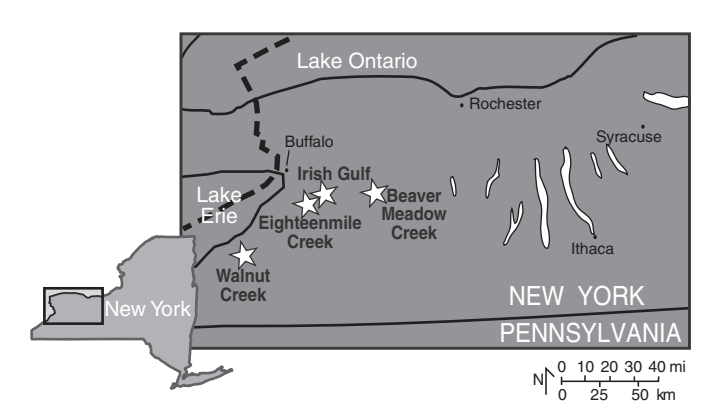


Fig. 1. Locality map of western New York, USA. Stars indicate sampling locations that trend most distal to most shoreward from west to east.

all geochemical analyses. Hand samples were cut perpendicular to the bedding plane to reveal ichnofabric and sedimentary structures (Fig. 2). Ichnofabric index values, as a method to quantify the amount of bioturbation, were determined on a cm-scale through each of our measured sections (Figs. 3–6). An ichnofabric index (i.i.) value of 1 indicates fully laminated sediments with all original sedimentary structures preserved. An i.i. of 5 represents a nearly homogenized fabric with completely disturbed bedding while retaining discrete burrows (Droser and Bottjer, 1986). Each value is interpreted to reflect different relative bottom water oxygen levels from anoxic (i.i. 1) to oxygen-replete (i.i. 5), but this characterization is complicated under conditions of temporally varying redox.

As a complement to the trace fossil data, samples were powdered for whole rock trace metal analysis at cm intervals (Figs. 3–6). Approximately 400 mg of powdered sample were ashed at 850 °C for 12 h and then dissolved using standard procedures through a three acid (HNO $_3$, HF, HCl) total digestion. Samples were analyzed using a quadrupole ICP-MS (Varian 820MS) at the Interdisciplinary Elemental Measurement Facility at SUNY Oswego. Quantitative data for Ti, V, Cr, Mn, Fe, Ni, Cu, Zn, Mo, Ba, Re, Pb, and U were acquired, and mean reproducibility of sample solution analyses (repeat measurement of the same solution) over the full range of concentration encountered was \pm 11%.

Highly reactive iron (Fe $_{HR}$) was calculated as the sum of Fe as pyrite, carbonate, and oxides—Fe $_{py}$, Fe $_{carb}$, and Fe $_{ox}$, respectively. Pyrite sulfur concentrations from standard chromium reduction methods (Canfield et al., 1986) were used to calculate Fe $_{py}$ assuming a stoichiometry of FeS $_2$. Fe $_{carb}$ and Fe $_{ox}$ were extracted sequentially as described by Poulton and Canfield (2005). Specifically, approximately 100 mg from 19 samples (4 from WC, 3 from EMC, 6 from IG, and 6 from BMC) were extracted sequentially: 1 M sodium acetate extraction adjusted to pH = 4.5 for 48 h with constant shaking (Fe $_{carb}$) followed by extraction of the sample residue for its iron oxide content (Fe $_{ox}$) using 50 g/L sodium dithionite buffered to pH = 4.8 for 2 h while shaking. All extracts were diluted 100-fold in 2% HNO $_3$ and analyzed for Fe concentrations using ICP-MS at UC Riverside.

For organic geochemical analysis, the exterior of each whole rock was removed to reduce potential contamination from any environmental hydrocarbon exposure and to remove any weathered material. These samples were cut into cm-thick fragments, which were then cleaned by sonication in a sequence of deionized water, methanol, and dichloromethane (DCM). Cleaned fragments were powdered in a shatterbox, and 5 g of crushed rock for each sample was extracted in a CEM Microwave Accelerated Reaction System (MARS) to produce bitumen extract. Full procedural blanks with combusted sand were run in parallel. The saturates, aromatics, and polar fractions of the bitumen were obtained by silica gel column chromatography, and biomarkers were quantitatively analyzed in both full scan and via single ion monitoring methods using gas chromatography—mass spectrometry (GC—MS) at UC

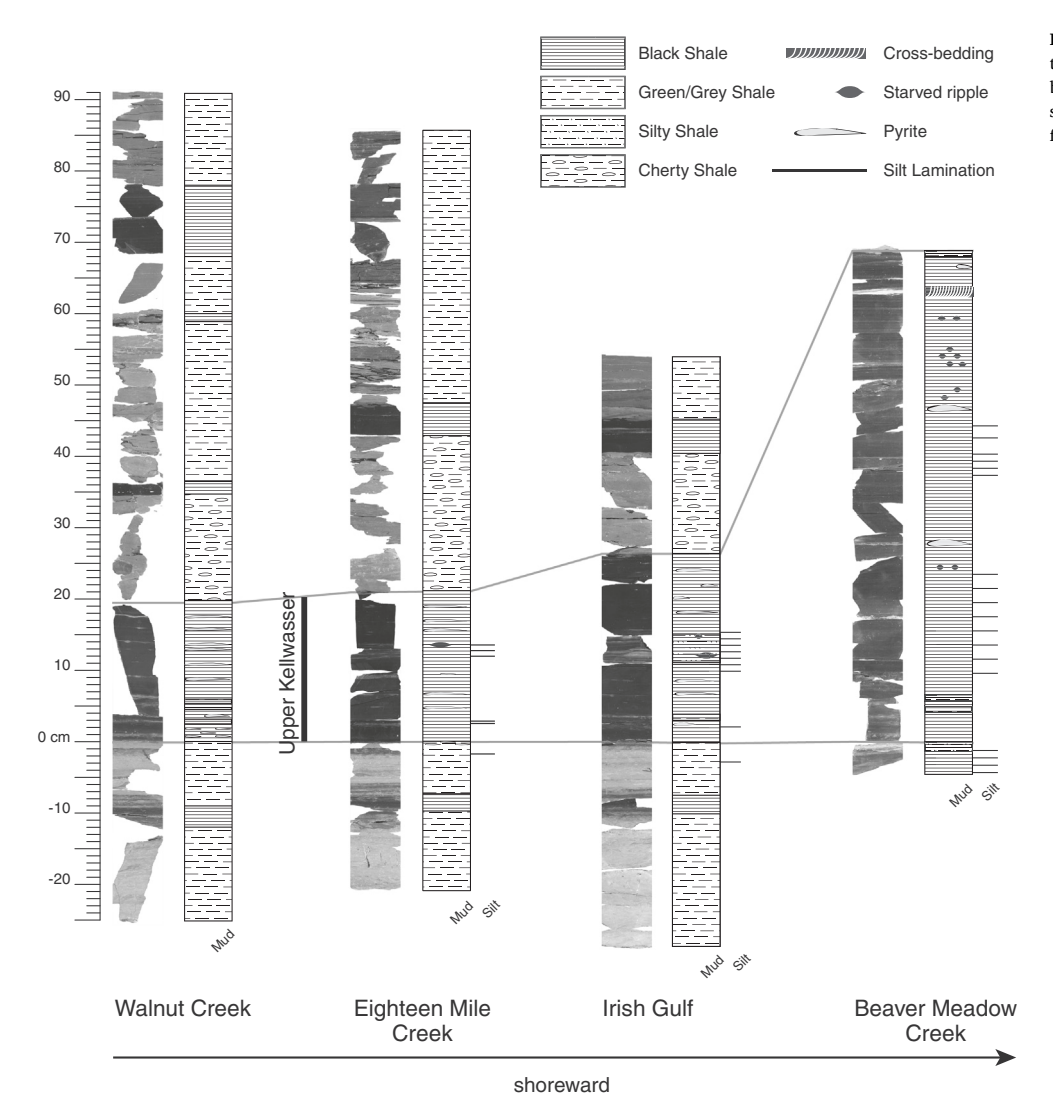


Fig. 2. Composite columns of hand samples through the Point Gratiot Bed (UKw-equivalent black shale) at the four localities sampled for this study, including respective stratigraphic sections for lithology and lithologic features.

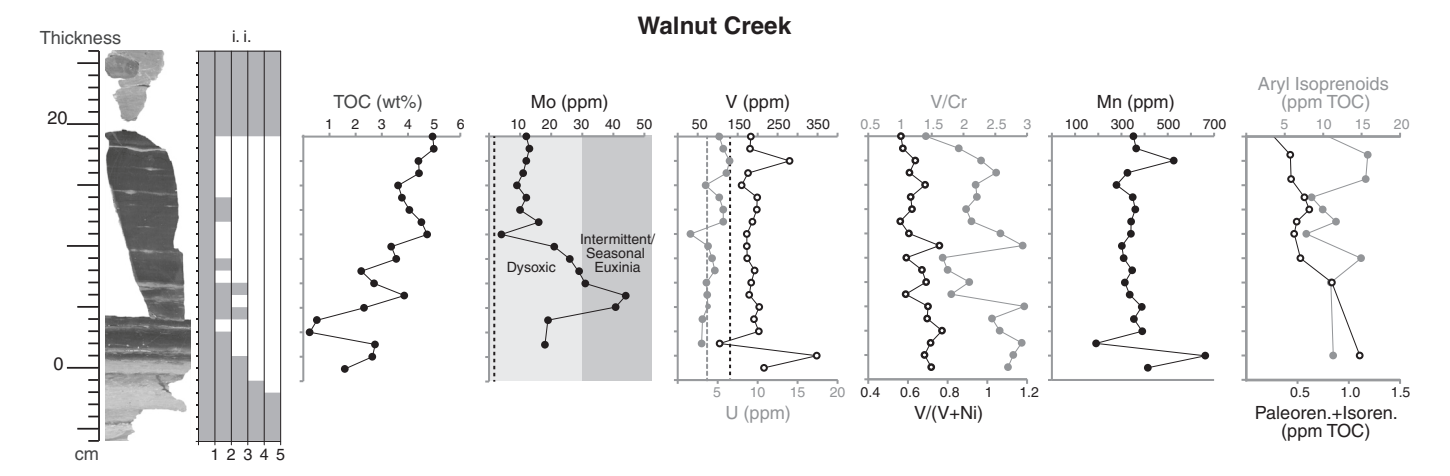


Fig. 3. Composite chemostratigraphic records of the UKw-equivalent (PGB) black shale for Walnut Creek section; from left to right: cm-scale, sedimentary column, ichnofabric index values, total organic carbon, molybdenum concentrations, uranium (closed circles) and vanadium (open circles) concentrations, V/(V + Ni) values (open circles) and V/Cr ratios (closed circles), manganese concentrations, aryl isoprenoid abundances (closed circles) and summed paleorenieratane and isorenieratane abundances (open circles). Vertical dotted lines indicate average shale values of each trace element: Mo = 2 ppm, U = 3.7 ppm, V = 130 ppm, Mr (not shown) = 850 ppm (Wedepohl, 1971, 1991). Shaded background on the Mo plot indicates ranges of Mo concentrations in modern sulfidic environments (from Scott and Lyons, 2012; 0–30 ppm = dysoxic, non-euxinic settings where sulfide is restricted to pore waters throughout the year; 30–100 ppm = intermittently/seasonally euxinic settings and the Mo-depleted Black Sea; > 100 pm = permanently euxinic, Mo-replete settings).

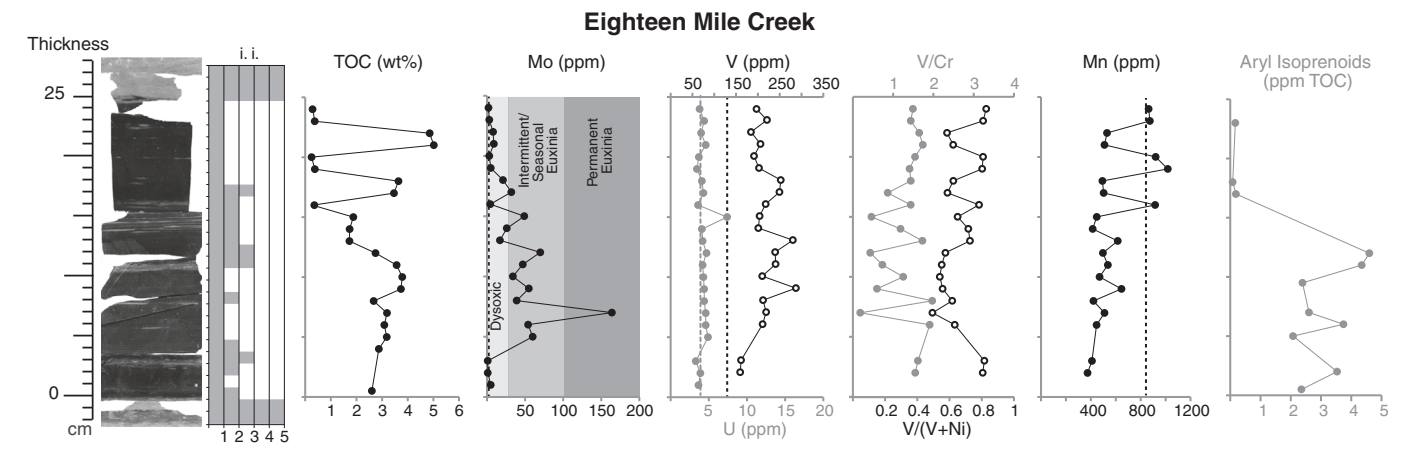


Fig. 4. Composite chemostratigraphic records of the UKw-equivalent (PGB) black shale for Eighteenmile Creek section; from left to right: cm-scale, sedimentary column, ichnofabric index values, total organic carbon, molybdenum concentrations, uranium (closed circles) and vanadium (open circles) concentrations, V/(V + Ni) values (open circles) and V/Cr ratios (closed circles), manganese concentrations, and aryl isoprenoid abundances. Vertical dotted lines indicate average shale values of each trace element: Mo = 2 ppm, U = 3.7 ppm, V = 130 ppm, Mn = 850 ppm (Wedepohl, 1971, 1991). Shaded background on the Mo plot indicates ranges of Mo concentrations in modern sulfidic environments (from Scott and Lyons, 2012; 0–30 ppm = dysoxic, non-euxinic settings where sulfide is restricted to pore waters throughout the year; 30-100 ppm = intermittently/seasonally euxinic settings and the Modepleted Black Sea; V/(V + Ni) values (open circles) and V/Cr ratios (closed circles), manganese concentrations, V/(V + Ni) values (open circles) and V/Cr ratios (closed circles), manganese concentrations, V/(V + Ni) values (open circles) and V/Cr ratios (closed circles), manganese concentrations, V/(V + Ni) values (open circles) and V/Cr ratios (closed circles), manganese concentrations, V/(V + Ni) values (open circles) and V/Cr ratios (closed circles), manganese concentrations, V/(V + Ni) values (open circles) and V/Cr ratios (closed circles), manganese concentrations, V/(V + Ni) values (open circles) and V/Cr ratios (closed circles), manganese concentrations, V/(V + Ni) values (open circles) and V/Cr ratios (closed circles), manganese concentrations, V/(V + Ni) values (open circles) and V/Cr ratios (closed circles), manganese concentrations, V/(V + Ni) values (open circles) and V/(V + Ni) va

Riverside. Thermal maturity was independently constrained from Rock-Eval pyrolysis, and the resulting parameters (Hydrogen Index, T_{max}) showed that these rocks were in the peak oil window and thus suitable for detailed biomarker analyses. For complete organic geochemical methods and screening criteria, see Haddad et al. (2016).

Total organic carbon (Figs. 3–6) was calculated as the difference between total carbon (TC) and total inorganic carbon (TIC), as measured using an ELTRA CS 500 carbon–sulfur analyzer equipped with acidification and furnace modules at UC Riverside. Standards AR4012 (limestone, 11.97% carbon) and AR4018 (soil, 1.26% carbon) were used for calibration, and average error was \pm 2% for TC and \pm 4% for TIC.

Investigation of ichnofabric allows for recognition of subtle variations in reduced but non-zero oxygen levels, parsing oxic conditions (generally > 2~mL/L dissolved $O_2)$ that are supportive of fully aerobic function from dysoxic conditions (traditionally > 0~mL/L but < 2~mL/L L $O_2)$ that are supportive of soft-bodied or poorly calcified benthic or

infaunal dysaerobic organisms (Rhoads and Morse, 1971; Byers, 1977; Thompson et al., 1985; Allison et al., 1995). We recognize that the term 'dysoxic' does not carry specific relevance in the geochemical community, which tends to favor 'suboxic' (but see Canfield and Thamdrup, 2009), and we feel that the historical oxygen limits assigned to dysoxia should be reconsidered in light of recent ecological studies of oxygen minimum zones (Levin, 2003; Woulds et al., 2007; Sperling et al., 2013; Sperling et al., 2016), but we use dysoxic in this paper in reference to our geochemical proxies to connote very low but unspecified values of dissolved O₂ in the bottom waters with pore waters that are often, but not always, rich in dissolved sulfide. Lipid biomarkers and trace metals, while less sensitive than the trace fossils to fluctuations under dysoxic conditions because of their more complex association with dissolved oxygen and greater influence from post-depositional processes, can nonetheless provide unambiguous evidence for anoxic and/or euxinic conditions during deposition of UKw-equivalent PGB. The different proxies used in tandem help distinguish among the competing water

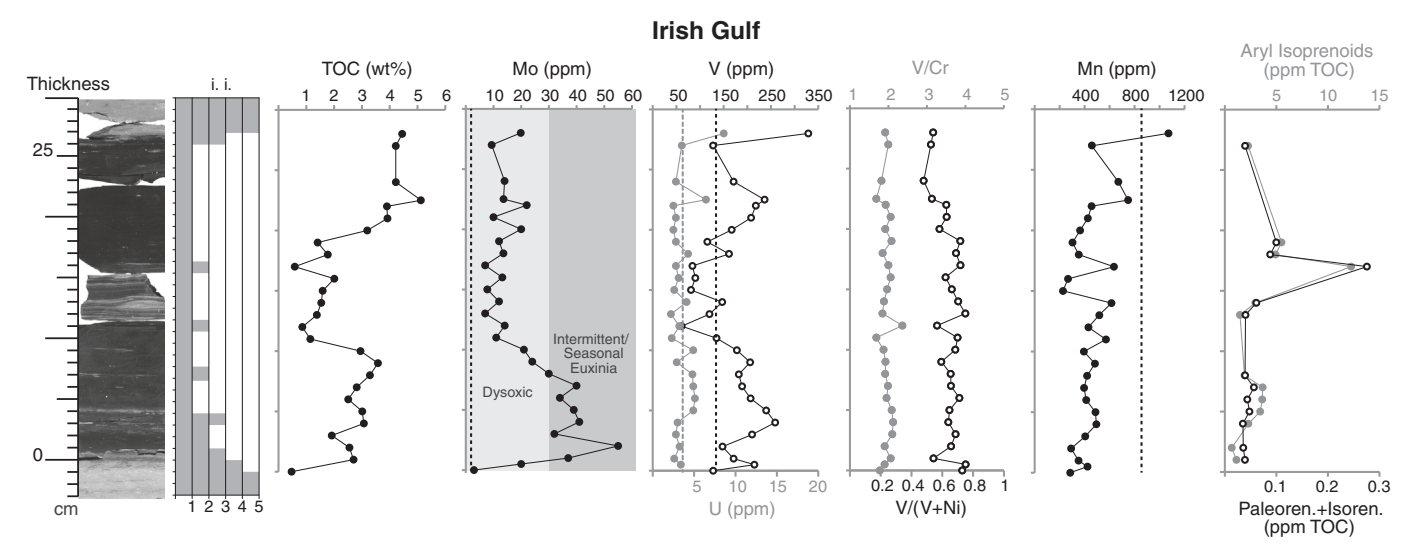


Fig. 5. Composite chemostratigraphic records of the UKw-equivalent (PGB) black shale for the Irish Gulf section; from left to right: cm-scale, sedimentary column, ichnofabric index values, total organic carbon, molybdenum concentrations, uranium (closed circles) and vanadium (open circles) concentrations, V/(V + Ni) values (open circles) and V/Cr ratios (closed circles), manganese concentrations, aryl isoprenoid abundances (closed circles) and summed paleorenieratane and isorenieratane abundances (open circles). Vertical dotted lines indicate average shale values of each trace element: Mo = 2 ppm, U = 3.7 ppm, V = 130 ppm, Mn = 850 ppm (Wedepohl, 1971, 1991). Shaded background on the Mo plot indicates ranges of Mo concentrations in modern sulfidic environments (from Scott and Lyons, 2012; 0–30 ppm = dysoxic, non-euxinic settings where sulfide is restricted to pore waters throughout the year; 30–100 ppm = intermittently/seasonally euxinic settings and the Mo-depleted Black Sea; > 100 pm = permanently euxinic, Mo-replete settings).

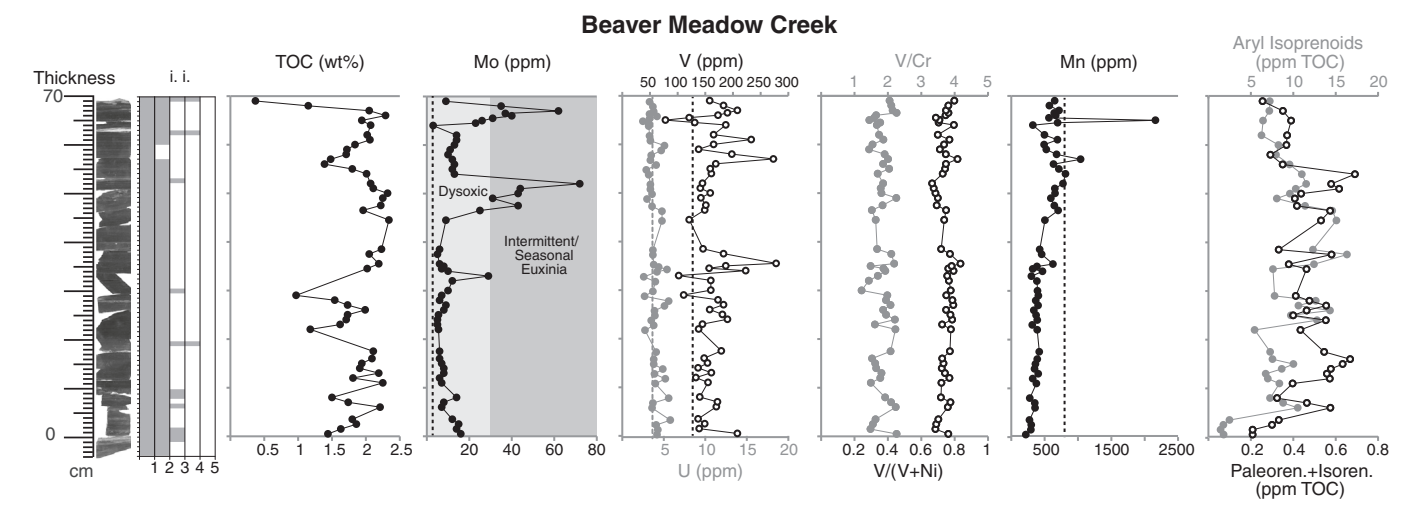


Fig. 6. Composite chemostratigraphic records of the UKw-equivalent (PGB) black shale for the Beaver Meadow Creek section; from left to right: cm-scale, sedimentary column, ichnofabric index values, total organic carbon, molybdenum concentrations, uranium (closed circles) and vanadium (open circles) concentrations, V/V + Ni) values (open circles) and V/Cr ratios (closed circles), manganese concentrations, aryl isoprenoid abundances (closed circles) and summed paleorenieratane and isorenieratane abundances (open circles). Vertical dotted lines indicate average shale values of each trace element: V/V/Cr Mo V/V/Cr Mo

column redox models for Devonian epeiric seas, which range from a high TOC oxic end member with intermittently dysoxic-anoxic bottom waters (Arthur and Sageman, 1994; Gallego-Torres et al., 2007; Pattan and Pearce, 2009), to an expanded oxygen minimum zone (Lüning et al., 2003; Murphy et al., 2000a; Marynowski et al., 2011; Algeo et al., 2011), to a deep water anoxic/euxinic end member (after Brown and Kenig, 2004, and Melendez et al., 2012).

3. Results and discussion

3.1. Biological signals of episodic bottom water oxygenation

Devonian trace fossils in shales representing deposition in low oxygen settings are typically horizontal to sub-horizontal, small or diminutive, not distinct, and often recognizable only because they disturb the original sedimentary fabric. It has been demonstrated, however, that trace fossil size, relative amount of bioturbation, and ichnofabric index can be used to infer relative bottom water oxygen on a microstratigraphic scale (Boyer and Droser, 2009, 2011) because the amount of biotic disruption to the original sedimentary fabric can be correlated to a relative oxygen level (Savrda and Bottjer, 1986, 1989; Savrda, 1992). Ichnofabrics are critical for demonstrating the presence of metazoans and corresponding implications for oxygen chemistry in the water column, even in the absence of body fossils, and they provide an independent paleoenvironmental context as a complement to the geochemical redox proxy records.

Due to the expanded nature of the PGB at BMC (measuring nearly 70 cm in thickness), we did not collect continuously on the cm-scale above and below the UKw event bed, but the stratigraphy, lithology, and biological traces tracked well across the three more distal localities (WC, EMC, and IG) before, during, and after the deposition of the UKw shale. Preceding the PGB at each of these localities are fully bioturbated silty green-gray shales containing a diverse assemblage of ichnogenera, commonly preserved as pyritized burrows, including *Skolithos, Thalassinoides*, and *Chondrites*, but predominantly *Planolites*. These ichnogenera, in association with an ichnofabric index of 5, indicate fully oxygenated bottom water conditions. Immediately preceding the PGB is a 2–3 cm thick precursor black shale bed (PBSB), which has been interpreted to record a rapid shift from fully oxygenated to anoxic bottom water conditions because of the abrupt termination of the pyritized burrows without evidence for an erosional contact with

laminated black shale. Following this PBSB, and leading into the PGB, is 10 cm of fully mottled ichnofabric only sparsely populated by discrete larger burrows. This facies is interpreted to represent an oxygenstressed dysoxic interval that led into the more anoxic UKw event (Boyer et al., 2014); remarkably similar variations in ichnofabric are also recorded through the UKw horizon in the Holy Cross Mountains of Central Poland (Stachacz et al., 2017).

The PGB black shale units do not preserve consistent i.i. values of 1, however, as would be expected for deposition under a persistently anoxic water column. Instead, the i.i. values fluctuate between 1 and 3 at IG, EMC, and WC. At the most proximal section (BMC), i.i. values reach 4, indicating biological disturbance of up to 60% of the original sedimentary fabric (Figs. 3-6). These occurrences of i.i. 4 are interpreted to represent the highest relative oxygen levels in the PGB. Few discrete trace fossils are captured in the PGB. Where recognized, they are identified as likely Planolites, measuring no more than a few mm wide and deep; no Skolithos or Chondrites are recognized in the UKwequivalent interval. At the top of the PGB at each locality are large, > 1 cm wide Thalassinoides burrows that penetrate as much as 5 cm from the overlying green-gray shale, which fills the burrows. These burrows mark a return to fully oxygenated conditions and are interpreted to represent a rapid re-oxygenation event based on erosional surfaces and the large burrows piping into laminated intervals.

Heterolithic bedding, facilitated by variable clay and silt content, characterizes the PGB at each locality; within the first 10 cm of UKwequivalent deposition are nearly cm-thick bioturbated green-gray shale laminae displaying i.i. values of 3. Several sedimentary structures are common to each locality, including lenticular bedding, where increased silt input produced abundant silt laminae, and starved ripples at EMC, IG, and BMC, capped by a cm-thick cross-bedding at BMC (Fig. 7). Lenticular bedding, starved ripples, and cross-stratification are most likely to have been formed by clear-water bottom currents rather than by turbidity currents (Shanmugam et al., 1993). These structures, products of traction and suspension deposition, are therefore interpreted to reflect episodic enhancement of bottom current energy and possible concomitant increases in benthic dissolved oxygen levels, especially in light of the ichnofabric evidence for intermittent colonization of the seafloor during the deposition of the UKw.

The level of biological sedimentary disruption associated with an i.i. of 2 does not suggest fully oxygenated conditions or colonization by larger macrofauna— an interpretation consistent with the paucity of

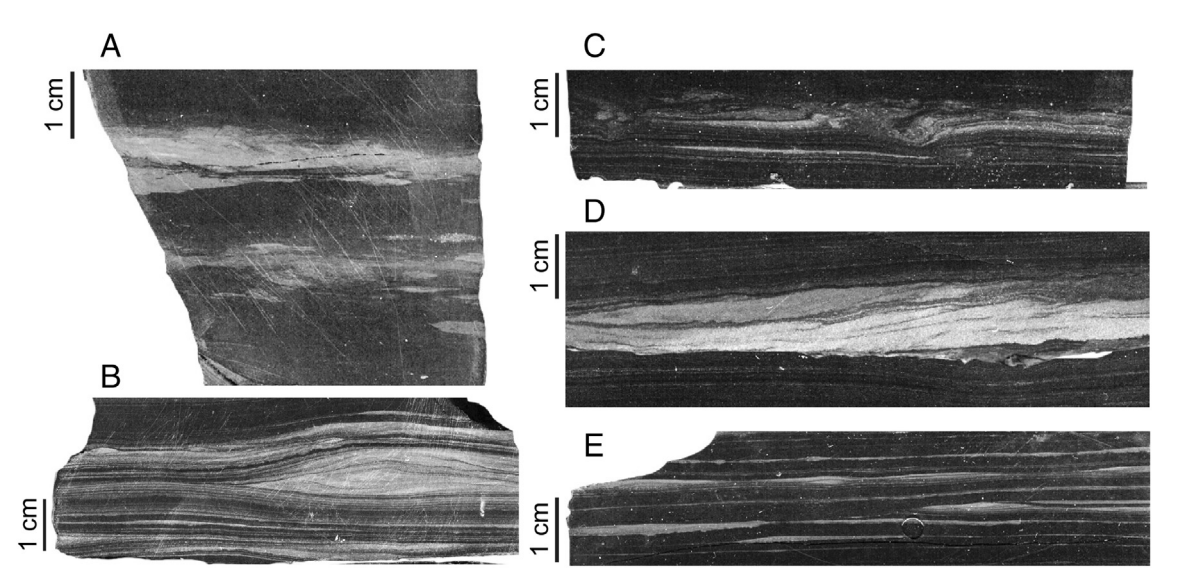


Fig. 7. Range of sedimentary structures displayed in polished hand samples of the Point Gratiot Bed; A) Walnut Creek, 87–90 cm: silt laminations disrupted by biological activity, i.i. 1–3; B) Irish Gulf, 120–123 cm: cm-thick starved ripple, i.i. 1; C) Eighteenmile Creek, 15.5–17 cm: deformed silt laminations displaying evidence of biological disruption, i.i. 2–3; D) Beaver Meadow Creek, 62–64 cm: cm-thick silt crossbedding, i.i. 2–4; E) Eighteenmile Creek, 14–16.5 cm: lenticular bedding and disturbed silt laminae, i.i. 2. Solid black bars = 1 cm.

large, discrete burrows. Bioturbation associated with i.i. 3 or 4, however, especially in conjunction with interbedded gray-green shale, was most likely caused by autochthonous macrofauna given the lack of evidence for turbidity currents that might have otherwise brought in allochthonous benthic fauna from shallower waters (Ozalas et al., 1994); this interpretation is consistent with evidence for opportunistic colonization by benthic fauna during deposition of the end-Famennian Hangenberg black shale (Marynowski et al., 2012). Because the alternating sequences of black and green-gray shale, on the scale of meters to tens of meters, are attributable to transgressive-regressive cycles (Johnson et al., 1985; Johnson and Klapper, 1992; Day, 1998; Over, 2002), it is probable that the oxygenation events within the UKw were a result of shorter-term changes in basin circulation patterns. Occurrences of i.i. 2 may indicate seasonal or event-induced (i.e., storms or turbidites) fluctuations of bottom water oxygen, when scattered, diminutive fauna disrupted sediments for a limited time. The periods of greater oxygenation, as indicated by i.i. values of 3 or 4 and with implications for short-term recolonization, were presumably facilitated by oxygenation events on time scales longer than subannual (Wetzel and Uchmann, 1998).

3.2. Iron speciation framework for variable redox

Major and minor element concentrations are key to understanding the redox state of the depositional environment of the PGB, and Fe species are the most effective proxies for euxinia (free sulfide in the water column) on a local scale (Lyons et al., 2009; Reinhard et al., 2012). We examined the Fe mineral speciation pattern in a subset of samples across the Appalachian Basin at each of our localities as a framework for understanding the more detailed and finely sampled trace metal patterns (Section 3.3). Iron enrichment patterns are well understood in modern sediments and have proven applicability in Devonian black shales for recognizing persistent and rapidly varying relative bottom water oxygen levels (Murphy et al., 2000a, 2000b; Werne et al., 2002; Sageman et al., 2003; Boyer et al., 2011). The method can reveal conditions ranging from euxinic to anoxic to dysoxic (reduced but non-zero oxygen); sediments with elevated ratios of reactive Fe (Fe_{HR}) to total Fe (Fe_T) compared with modern and ancient oxic marine sediments record anoxic and euxinic conditions (Raiswell and Canfield, 1998; Poulton and Canfield, 2011). FeHR includes iron mineral phases that have the potential to react with dissolved hydrogen sulfide during deposition in the water column or early diagenesis (carbonates and

oxides) (Raiswell and Canfield, 1998) summed with iron already present as pyrite. Modern oxic sediments preserve a range of Fe_{HR} from 0.06 to 0.38, and Fe_{HR}/Fe_{T} ratios exceeding \sim 0.38 are interpreted to reflect deposition in an anoxic setting (Poulton and Canfield, 2011; Reinhard et al., 2012).

For anoxic samples with Fe_{HB}/Fe_{T} ratios exceeding ~ 0.38 , the degree to which the highly reactive Fe pool has been pyritized, expressed as Fe_{py}/Fe_{HR}, can be used to distinguish between systems buffered by Fe (II) versus H2S (e.g., whether anoxic water column was ferruginous or euxinic). Near-complete pyritization of the highly reactive iron pool indicates an excess of dissolved H2S in the anoxic system and scavenging of reactive Fe as pyrite (Poulton and Canfield, 2011). More specifically, values of $Fe_{pv}/Fe_{HR} > 0.8$ (80% pyritization) provide compelling evidence for euxinia when coupled with FeHR/FeT evidence of an anoxic water column (reviewed in Lyons and Severmann, 2006; Poulton and Canfield, 2011). Fig. 9 places the 19 samples that were processed for Fe species on a Fe_{HR}/Fe_{T} versus Fe_{Pv}/Fe_{HR} crossplot, on which Fe_{HR}/Fe_T values < 0.38 suggest oxic deposition. Fe_{HR}/Fe_T values for the PGB samples (mean = 0.43, modestly in excess of the threshold value of 0.38 for anoxic bottom waters) range from 0.17 at Eighteenmile Creek to 0.78 at Beaver Meadow Creek, with samples from each of the four sections falling within the range displayed by modern oxic and anoxic sediments (Fig. 8; see also Table 1). Uniformly high Fe_{pv}/Fe_{HR} values (min = 0.88, max = 0.97, mean = 0.93) of the sample set suggest the presence of appreciable dissolved H₂S in either shallow sedimentary pore fluids, under oxic-dysoxic conditions (as indicated by lower FeHR/FeT and FeT/Al values), or in the water column associated with anoxic deposition.

Elevated Fe $_T$ /Al ratios, when compared with average continental crust values, can further distinguish anoxic and euxinic settings from oxic and low oxygen sites by accounting for Fe enrichment relative to average detrital input (generally Fe $_T$ /Al of 0.5 \pm 0.1; Lyons et al., 2003; Lyons and Severmann, 2006). Fe $_T$ concentrations in the PGB range from 3.39 to 6.40 wt%. Fe $_T$ normalized to continentally derived Al concentrations, however, produces values (mean = 0.61) ranging from 0.44 at Eighteenmile Creek, within the range of values attributed to oxic, typically bioturbated sediments (Lyons et al., 2003), to 1.17 at Beaver Meadow Creek, an extremely elevated value consistent with deposition within an anoxic water column (Table 1).

Duan et al. (2010) compared Fe content of samples of the Middle Devonian Oatka Creek and Upper Devonian Geneseo formations, which have been studied extensively for lithology, paleontology, and

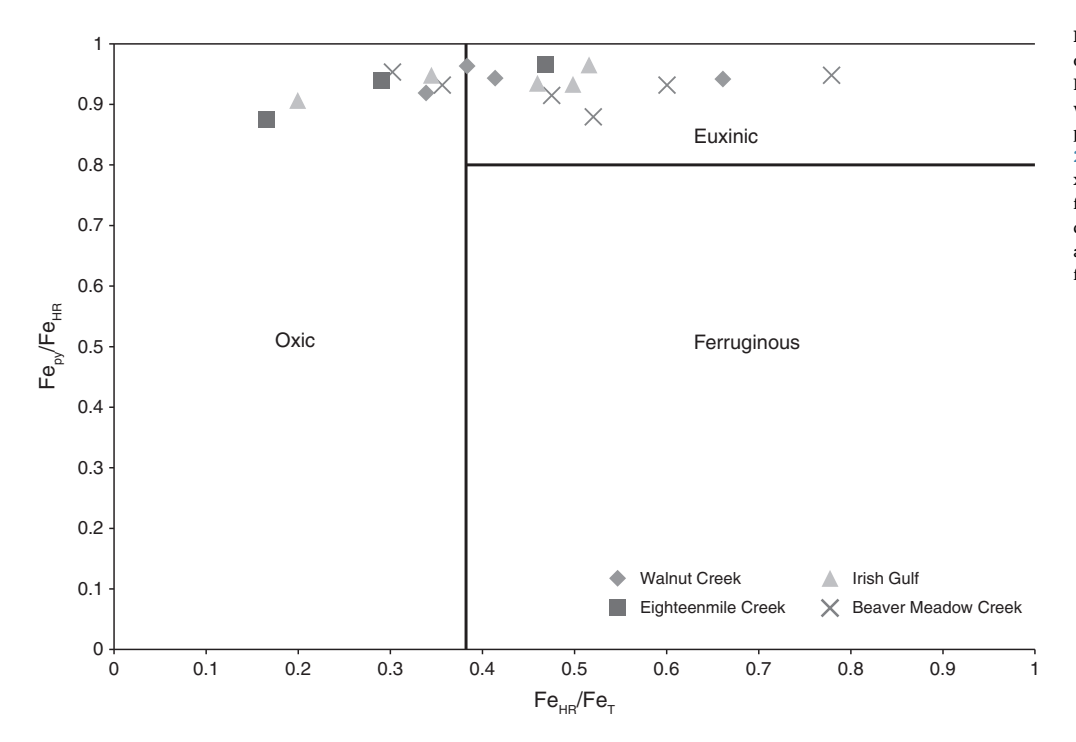


Fig. 8. Iron mineral speciation data displayed on a Fe_{HR}/Fe_{T} vs. Fe_{py}/Fe_{HR} crossplot. Fe_{HR}/Fe_{T} values ≤ 0.38 indicate oxic deposition; values > 0.38 indicate dysoxic/anoxic deposition (Raiswell et al., 2001; Reinhard et al., 2012). Fe_{py}/Fe_{HR} values > 0.8 indicate euxinic conditions with excess H_2S to scavenge for pyrite formation, while values < 0.8 indicate ferruginous conditions with a large reactive Fe reservoir but limited or nonexistent free H_2S (Lyons and Severmann, 2006).

Table 1
Fe speciation for select samples, arranged stratigraphically by locality.

Sample	Strat. Ht. ^a (cm)	FeT ^b wt%	Fe _T /Al ^c	$\mathrm{Fe_{HR}}^{\mathrm{d}}/\mathrm{Fe_{T}}$	$\mathrm{Fe_{py}}^{\mathrm{e}}/\mathrm{Fe_{HR}}$				
Beaver Meadow Creek									
BMC 67	67	4.85	0.74	0.36	0.93				
BMC 64	64	3.39	0.54	0.52	0.88				
BMC 52	52	6.40	1.17	0.78	0.95				
BMC 47.5	47.5	5.35	0.82	0.60	0.93				
BMC 16	16	3.52	0.54	0.48	0.91				
BMC 0.5	0.5	3.92	0.48	0.30	0.95				
Irish Gulf									
IG 107	27	4.59	0.62	0.46	0.93				
IG 113	21	5.05	0.61	0.46	0.93				
IG 117	17	3.79	0.45	0.20	0.91				
IG 123	11	3.51	0.69	0.50	0.93				
IG 127	7	4.05	0.56	0.52	0.97				
IG 133	1	3.90	0.49	0.34	0.95				
Eighteenmile Creek									
EMC 21	21	4.88	0.65	0.47	0.97				
EMC 15	15	3.76	0.44	0.29	0.94				
EMC 1	1	4.13	0.49	0.17	0.88				
Walnut Creek									
WC 74	19.5	5.44	0.79	0.66	0.94				
WC 78	15.5	3.90	0.52	0.41	0.94				
WC 84	9.5	3.86	0.51	0.34	0.92				
WC 88	5.5	4.03	0.54	0.38	0.96				

 $^{^{\}rm a}$ Strat. Ht. = stratigraphic height in cm above the base of the Upper Kellwasser black shale.

geochemistry (see Murphy et al., 2000a for the Geneseo; Werne et al., 2002 for Oatka Creek; and Sageman et al., 2003 for both). The authors documented a difference of Fe $_{\rm T}/{\rm Al}$ content between the two formations, both of which pre-date the PGB, with the Geneseo displaying Fe $_{\rm T}/{\rm Al}$ values between 0.41 and 0.62 and the Oatka Creek's Fe $_{\rm T}/{\rm Al}$ values ranging from 0.35 to 1.23. Further, they characterized differences in depositional redox conditions for these two black shale units based on

their Fe chemistry, TOC content, sedimentary fabric, and redox sensitive trace metal enrichments.

Specifically, Duan et al. (2010) asserted that the Oatka Creek Formation accumulated under a dominantly euxinic water column, whereas the Geneseo Formation was deposited at a time that the Appalachian Basin was less reducing and only intermittently euxinic (consistent with the conclusions of Murphy et al., 2000a; Werne et al., 2002; and Sageman et al., 2003). Furthermore, ecological and sedimentological evidence from the Geneseo Formation, including sedimentary structures indicative of diverse modes of sediment transport and deposition, bioturbation up to i.i. 3, and an array of dysaerobic fauna and ichnogenera (Boyer and Droser, 2007, 2009; Wilson and Schieber, 2015), points to deposition under conditions more energetic than would be expected of a stagnant, pervasively anoxic basin. We argue here using similar lines of evidence—Fe speciation data in concert with ichnofabrics, trace metals, and lipid biomarkers-that the PGB was deposited in a variable redox regime that was less reducing and only intermittently euxinic and therefore more similar to the depositional setting of the Geneseo Formation than the dominantly euxinic Oatka Creek Formation.

3.3. Trace metal signals of intermittent euxinia

Trace metals (e.g., Mo, V, U, Zn, Ni, Pb, Cu, Co, and Cr) have demonstrated utility as marine redox proxies, and their concentrations are commonly used to infer variations in bottom water oxygen content and, more specifically, variations in the concentration of water column sulfide (Arthur and Sageman, 1994; Wignall, 1994; Rimmer, 2004; Algeo and Maynard, 2004; Tribovillard et al., 2006). Molybdenum has specifically been employed to document variations in bottom water oxygen levels in Devonian black shales from New York State, and high-resolution fluctuations in sedimentary Mo concentrations have been shown to be useful for extrapolating relative paleo-oxygen levels on a cm vertical scale (Boyer et al., 2011).

Molybdenum levels are enriched above crustal values (ca. 1–2 ppm) under persistently oxygen deficient settings (Morford and Emerson, 1999; Scott et al., 2008) and typically highly enriched beneath euxinic waters (Calvert and Pederson, 1993; Lyons et al., 2003). However, sedimentary Mo contents between \sim 2 and 30 ppm are recognized

^b Fe_T = total Fe content.

 $^{^{\}rm c}$ Fe $_{\rm T}/{\rm Al}$ = total Fe content standardized to detrital Al input.

 $[^]d$ Fe_{HR} = highly reactive iron calculated from Fe_{py} + Fe_{carb} + Fe_ox (pyrite, ferrous carbonates, ferrous oxides, respectively).

^e Fe_{pv} = iron species present as pyrite.

beneath dysoxic waters (McManus et al., 2006; Scott and Lyons, 2012), where sulfide is limited to pore waters. Intermittent/seasonal euxinia can result in values on the high end of this range or higher depending on water column Mo availability and the persistence of euxinia (Murphy et al., 2000a; Lyons et al., 2009; Scott and Lyons, 2012). Greatly enriched Mo values (in excess of 100 ppm) are interpreted to represent permanent euxinia in Mo-replete settings (Werne et al., 2002; Sageman et al., 2003; Algeo and Lyons, 2006; Gordon et al., 2009; Scott and Lyons, 2012).

Molybdenum enrichments in the PGB at these four localities average 20 ppm (min = 1 ppm; max = 164 ppm; mean crustal value = 2 ppm; Figs. 3-6). Irish Gulf, Eighteenmile Creek, and Walnut Creek, the three most distal localities, share a distinctive stratigraphic pattern, with Mo values enriched (up to 44 ppm at WC, 164 ppm at EMC, and 55 ppm at IG) in the bottom half of the UKw depositional sequence and more depleted values between 2 and 49 ppm in the top half. It is important to note that one outlier sample that defines a Mo enrichment excursion at EMC (164 ppm at cm 7) is more than twice the concentration of the next highest enrichment value, a value of 72 ppm observed at BMC, and unequivocally points to permanent euxinia in a Mo-replete setting (Fig. 4). The exceptionally high Mo enrichment of sample EMC 7 clearly indicates ample Mo availability at the onset of PGB deposition, underscores the importance of our cm-scale sampling scheme, and suggests dramatic redox fluctuations on a fine scale that would be overlooked by coarser sampling.

A different stratigraphic pattern is displayed in the expanded section at Beaver Meadow Creek, where Mo concentrations remain low (mean = 9 ppm; max = 29 ppm) for the first 45 cm of UKw deposition and then spike to maxima of 72 ppm and 62 ppm in two excursions in the top 20 cm of deposition (Fig. 5). This stratigraphic progression suggests that the PGB at BMC was deposited under a Mo-replete water column and likely reflects fluctuating local redox conditions because the Mo excursions roughly track with high TOC, increases in V, higher concentrations of green sulfur bacteria markers, and euxinic Fe ratios.

Enrichment patterns for Mo captured in sediments can be strongly dependent on the reservoir concentration of Mo in the water column, which may be limited in a restricted basinal setting (Algeo and Lyons, 2006). However, the BMC data appear not to be reflective of the basin reservoir effect and a lack of available Mo, and very high (> 200 ppm) Mo values found in correlative strata in the Madre de Dios Basin, Bolivia, imply that the global dissolved Mo inventory remained high throughout the UKw deposition (Tuite, M., pers. comm.). It is less clear how Mo availability affected the muted enrichments documented from WC, EMC, and IG, where increased TOC contents toward the top of the PGB correspond inversely with diminished Mo concentrations, especially in the few samples where anoxic FeHR/FeT values contrast with dysoxic-oxic values of Mo (Table 1). While we cannot rule out that episodic depletions in local marine inventories could have influenced the magnitude of Mo enrichments in these samples (Algeo, 2004) as a secondary factor, the other paleontological and geochemical proxies employed to test the PGB depositional model point away from trace metal inventory as the dominant constraint of our data. Instead, the overall trace metal systematics argue for variable marine redox conditions as the major control on the sedimentary Mo concentrations in the Appalachian Basin Upper Kellwasser, since muted but not full enrichments for both anoxic (Mo, V, U) and oxic (Mn) depositional settings were found consistently through the strata and are complemented by oxic-dysoxic Fe species and ichnofabrics.

Importantly, these observed patterns indicate that Mo concentrations do not remain consistently enriched throughout deposition of UKw-equivalent black shale in the Appalachian Basin, but rather can fluctuate dramatically on a cm-scale. This relationship demonstrates the utility of a high-resolution approach because we are able to capture variability that coarser sampling would miss. Furthermore, Mo enrichment levels are lower than those documented from pervasively euxinic settings, which are consistently in excess of 60 ppm and

occasionally > 100s of ppm (Scott and Lyons, 2012). Many of the measured Mo values fall within the range for deposition under a dysoxic/suboxic water column (i.e., dissolved sulfide is restricted to the sediments; Scott and Lyons, 2012), and excursions in Mo enrichment suggest only intermittently euxinic conditions during deposition of the UKw. Additionally, the uniformly low to moderate TOC values measured in our sections (0.24–5.53 wt%; mean = 2.62 wt%; Figs. 3–6), which are comparatively organic-lean for Devonian black shales and do not correlate significantly with measured sedimentary Mo concentrations, are also consistent with fluctuating redox conditions (Sageman et al., 2003; Algeo and Lyons, 2006; Algeo et al., 2007).

Enrichment factors were also calculated for Mo to address the possibility that the observed stratigraphic trend might reflect patterns of dilution by CaCO₃, for example, rather than temporally varying controls on Mo uptake. The related trend (Supplementary Fig. 1) strongly resembles that of Mo (ppm) (Figs. 3–6), suggesting that dilution has not impacted our interpretations, and this assertion should extend to the other elements of interest, specifically U (Supplementary Fig. 2). The conclusions are the same when Mo and U concentrations are normalized to TOC content (not shown here).

Comparisons of enrichment patterns of various trace metals, specifically U, V, and Mo, may shed further light on coeval bottom water redox conditions, because U and V can accumulate under broadly anoxic conditions, while significant Mo sequestration requires free H2S. Enrichment in only U and V to the exclusion of Mo suggests deposition under dysoxic to anoxic conditions, whereas enrichment of U, V, and Mo necessarily reflects sulfidic conditions in the sediments or overlying water column (Algeo and Maynard, 2004). At all four localities, V is enriched to slightly higher than average shale values, comparable to Black Sea sediment enrichments (PGB average = 179 ppm; Figs. 3-6; Table 2). However, U is barely enriched above average shale and crustal values (PGB average = 4 ppm; Figs. 3-6; Table 2), while Mo, as discussed above, is moderately enriched in the PGB across western New York. Post-depositional loss of trace element enrichment is possible under conditions of vacillating redox, mobilizing authigenic elements and decreasing original enrichments, especially in environments where conditions vary relatively rapidly (e.g., via turbidite deposition or storm events; Tribovillard et al., 2006). Uranium is particularly sensitive to reoxidation and remobilization (Morford et al., 2001; McManus et al., 2005). Even if U accumulated under reducing conditions initially, the absence of U enrichment in the UKw-equivalent shales of the Appalachian Basin could imply post-depositional oxygen replenishment to the bottom waters on a rapid temporal scale (as evidenced from the Upper Devonian Rhinestreet Shale of western New York; Lash, 2016).

V/Cr and V/(V + Ni) have also been used as redox indicators for

Table 2
Minor elements in μg/g (parts per million).

Element	Average shale ^a	WC ^b Mean	EMC ^c Mean	IG ^d Mean	BMC ^e Mean
Ва	580	614	617	616	301
Cr	90	88	252	88	83
Cu	45	84	113	107	63
Mn	850	362	591	463	519
Mo	1	18	9	21	16
Ni	68	106	114	101	55
Pb	22	43	38	58	34
Re	0.01	0.004	0.003	0.006	0.002
U	3.7	4.5	4.2	3.6	3.8
V	130	195	216	171	163
Zn	95	64	224	95	113

^a Average shale data from Wedepohl (1971, 1991).

^b WC = Walnut Creek; data from this study.

^c EMC = Eighteenmile Creek; data from this study.

 $^{^{\}rm d}$ IG = Irish Gulf; data from this study.

^e BMC = Beaver Meadow Creek; data from this study.

black shale formation. Each relates V, a redox-sensitive element, to an element that is more strongly associated with the detrital fraction (Jones and Manning, 1994; Tribovillard et al., 2006). While Cr may be enriched under anoxic conditions, normalizing Cr content for the PGB samples to Ti yields an average value of 1.76 \times 10 2 (ppm/ppm) across the four localities, which is comfortably within the range of Phanerozoic average upper crust composition (Reinhard et al., 2013). Therefore, patterns of V/Cr variability likely reflect the redox sensitivity of V. Threshold values of these ratios have been described and are interpreted to correlate with oxic, dysoxic, and anoxic conditions (Hatch and Leventhal, 1992; Jones and Manning, 1994; Wignall, 1994; Rimmer, 2004). V/Cr values for our Appalachian Basin localities range from 0.18 (well within what would be interpreted as oxic levels) at Eighteenmile Creek to 2.96 (consistent with dysoxic conditions) at Walnut Creek (Figs. 3–6). V/(V + Ni) values display a similar range, from oxic values (min = 0.48, below the dysoxic/anoxic transition value proposed by Hatch and Leventhal, 1992) to values close to the euxinic threshold (max = 0.83; Figs. 3-6). Joachimski et al. (2001) measured V/Cr and V/(V + Ni) ratios across the F/F boundary in the Polish Kowala section. They reported V/Cr ratios consistently above 4.25 (the anoxic threshold; Jones and Manning, 1994) and as high as 18, and V/(V + Ni) ratios of approximately 0.8 (near the 0.84 euxinic threshold proposed by Hatch and Leventhal, 1992) through the UKw, consistent with the existence of anoxic conditions during UKw deposition at Kowala. A subsequent study at Kowala (Racki et al., 2002), however, yielded much lower V/Cr ratios (max. of approximately 2.1) supported by unreported low V/(V + Ni) ratios, indicating fluctuating bottomwater conditions leading to dysoxia in the early Famennian. Our data for western New York are comparably low and variable and suggest a similar interpretation to the Racki et al. (2002) study.

Manganese can be enriched even in weakly oxic (oxygen-limited) areas of marine deposition as oxide minerals and displays values well in excess of the crustal average (600 ppm) under oxygenated bottom waters (Calvert and Pederson, 1993), Enrichment of Mn has been linked to the position of the chemocline in the Black Sea (Lyons et al., 1993) and other low oxygen settings. Alternatively, pore water reduction and related remobilization of Mn can result in precipitation of Mn at the sediment-water interface beneath oxygenated bottom waters. While Mn values at WC, the most distal locality and condensed section, remain unenriched throughout the UKw sequence, Mn concentrations increase to values much greater than average shale values (850 ppm; Wedepohl, 1971, 1991) in the upper half of the PGB at EMC (max = 1018 ppm), IG (max = 1072 ppm), and BMC (max = 2161 ppm) (Figs. 3-6). Quinby-Hunt and Wilde (1994) defined four groups of black shales based on Fe-Mn-V contents, providing a range of average Mn values for anoxic black shales (Groups 2 and 3) of 170-310 ppm, very similar in value to Mn concentration minima in the PGB (from 191 ppm at WC to 374 ppm at EMC). Average Mn concentrations in the PGB range from 362 ppm (at WC) to 591 (at EMC), whereas maximum Mn concentrations from EMC, IG, and BMC fall within the range of average Group 1 oxic low-calcic shales (1300 ppm). Considered together, these data place the PGB black shales between fully anoxic and fully oxic Mn values. Muted enrichments of Mn relative to anoxic black shales are most likely attributable to enhanced Mn uptake associated with episodes of oxic deposition. It is noteworthy that maximum Mn enrichment at BMC, the most shoreward locality, is found between two Mo excursions and only 2 cm below the final Mo maximum near the end of deposition of the UKw-equivalent black shales (Fig. 5). These relations suggest a vertically migrating chemocline, including local episodic seafloor ventilation, and reinforce the dramatic redox variability we interpret from our proxies.

3.4. Biomarker record of photic zone euxinia

While the inorganic proxies capture redox variability at the sediment-water interface and in bottom water, lipid biomarkers can help fingerprint the spatial and temporal extension of the sulfidic water mass

into the uppermost water column. Specifically, the C₄₀ aromatic carotenoid pigment produced by Chlorobi, isorenieratene, is well-preserved in sediments as the molecular fossil isorenieratane and is used as a biomarker for photic zone euxinia in marine and lake surface waters (Summons and Powell, 1986; French et al., 2015). Isorenieratane and its diagenetic products, aryl isoprenoids, indicate that free hydrogen sulfide was present at least episodically in the photic zone during accumulation of these deposits. Chlorobi are strictly anaerobic, obligate phototrophs using mainly H₂S as a preferred electron donor for photosynthesis. While global-scale photic zone euxinia has been implied by previous biomarker studies of F/F boundary sediments in Europe, western Canada, Australia, and North America (Brown and Kenig, 2004), this interpretation has not been adequately constrained due to the localized nature of these studies and the tendency to concentrate analyses on organic-rich strata in productive continental margin settings and epeiric basins. Furthermore, Chlorobi carotenoid markers are commonly found in petroleum of all geological ages and are generally associated with euxinic conditions for organic-rich source rocks.

Chlorobi-derived biomarkers (the sum of C₄₀ isorenieratane and paleorenieratane plus their C13-C22 aryl isoprenoidal fragments) were identified at each locality at cm-scale, quantified to a suitable standard, and normalized to TOC. Isorenieratane and Paleozoic-specific marker paleorenieratane (Maslen et al., 2009; Melendez et al., 2013) were detected at levels slightly in excess of detection limits (0-0.73 ppm TOC; Figs. 2, 4-5) at three localities (WC, IG, and BMC), and a suite of aryl isoprenoids (C₁₃-C₂₂; Figs. 3-6) was measured in each PGB sample. The presence of aryl isoprenoids and trace levels of parent C40 carotenoids (isorenieratane and paleorenieratane) provide evidence for at least intermittent photic zone euxinia during the deposition of the Point Gratiot Bed, yet the low absolute abundance of Chlorobi markers and their relative contribution to preserved sedimentary organic matter must also be considered. Aryl isoprenoid abundances at the studied localities range from 0.08 to 16.3 ppm TOC and are generally low in magnitude (mean = 6.44 ppm TOC, n = 79). The highest abundances are documented from the most distal locality, WC (mean = 11 ppm TOC, max = 15.8 ppm TOC), and the most shoreward locality, BMC (mean = 9.04 ppm TOC, max = 16.3 ppm TOC). The greatest range of abundances is documented from BMC (1.44-16.3 ppm TOC, with a standard deviation of 3.53 ppm TOC).

Samples from above and below the PGB at WC and IG display a range of aryl isoprenoid concentrations similar to that recognized from the PGB (WC: 10.7–19.3 ppm TOC from five samples; IG: 0.76–6.83 ppm TOC from four samples). It is worth noting that the greatest concentrations of aryl isoprenoids of the four localities was measured in a sample collected from a thin black shale bed 17 cm below the Dunkirk Formation and 58 cm above the PGB at WC. The measured 19.3 ppm TOC aryl isoprenoid abundance of this layer correlates well with a measured high (101 ppm) Mo concentration for the same sample. This Mo concentration is over twice the concentration of the most-enriched WC PGB sample.

While all aryl isoprenoid abundances are roughly within the same order of magnitude through deposition of the PGB at the four localities, there is clear variability on the cm-scale through the PGB. At BMC, pre-PGB aryl isoprenoid abundances exceed 10 ppm TOC, diminishing to < 2 ppm TOC in the first 5 cm of PGB deposition (Fig. 5). The marked reduction of Chlorobi markers is not due to lower TOC values before the PGB, as TOC is roughly unchanging prior to and during deposition of the PGB. At IG, uniformly low and unchanging concentrations of aryl isoprenoids and C40 parent carotenoids (paleorenieratane + isorenieratane) are interrupted by a single sample that contains three times the concentration of Chlorobi markers compared to the samples above and below. In contrast, EMC aryl isoprenoid concentrations appear to have been enriched during accumulation of the lower half of PGB deposition but diminished to nearly undetectable levels as the upper half accumulated, tracking the overall Mo stratigraphic pattern.

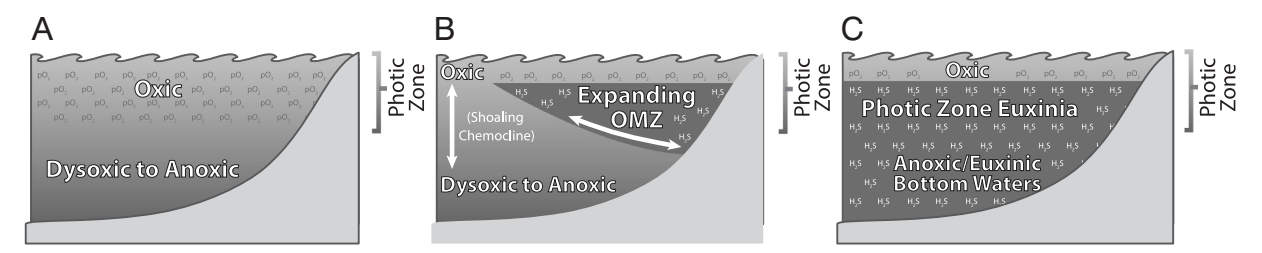


Fig. 9. Paleoenvironmental redox models for Late Devonian epeiric seas; A) oxic end member: an oxic setting with sub-oxic bottom waters and sulfide production confined to sedimentary pore waters; B) expanding OMZ (oxygen minimum zone) model: an expanding and contracting OMZ, dynamically maintained by respiration of organic matter in a productive continental margin, resulting in a stratified marine redox column with only intermittent or seasonal photic zone euxinia (after Murphy et al., 2000a; Algeo et al., 2011; Marynowski et al., 2011); C) anoxic end member: a permanently oxygen stressed setting that includes a persistently euxinic water column extending into the photic zone (after Brown and Kenig, 2004, and Melendez et al., 2012).

The stratigraphic variability of Chlorobi carotenoid markers in the PGB contrasts with the stable biomarker stratigraphic profiles of saturated hydrocarbons at these localities as well as consistent durability of the primary producer community throughout accumulation of the black shale interval (Haddad et al., 2016). Detailed, cm-scale stratigraphy from many different biomarker compound classes shows that the overall microbial community structure reflected by biomarker assemblages was very similar among the four sections and changed little through the black shale study interval. Despite a fluctuating chemocline culminating in intermittent photic zone euxinia during episodes of elevated export production as evidenced by low absolute yields of Chlorobi carotenoid markers, sterane, hopane, and other polycyclic biomarker alkane distributions provide no obvious evidence of significant changes in planktonic microbial ecology or modes of primary production. Thus, the composition of organic matter exported from surface waters can be very stable during these black shale depositional events, while controlling local redox conditions in the waters beneath the photic zone. That is, a stable, productive planktonic microbial community yielding a persistent organic flux can dynamically maintain an oxygen minimum zone (Fig. 9).

The low abundances of summed aryl isoprenoids detected in the PGB are similar in concentration to those reported from the middle Famennian of Poland, a succession that does not correlate with a significant bioevent (max: 5.2 ppm TOC; Marynowski et al., 2007). Low aryl isoprenoid concentrations of the Polish strata were attributed to episodic photic zone euxinia. Total aryl isoprenoid concentrations (C₁₃-C₂₂) in the Polish Kowala quarry range from 2.78 to 23.74 ppm TOC (Marynowski et al., 2011) in the Palmatolepis triangularis conodont zone that immediately overlies the PGB in the Appalachian Basin and marks the transition from the Frasnian to the Famennian (Over, 2002). The aryl isoprenoid concentration from a sample collected from lowermost Famennian strata in the Polish Kowala quarry is 11.75 ppm TOC, similar in value to the aryl isoprenoid mean at the WC locality of the present study. Marynowski et al. (2011) interpreted the early Famennian paleoenvironmental conditions of Poland to have been intermittently euxinic in the oxygen minimum zone and suboxic to weakly anoxic at the seafloor. Episodes of photic zone euxinia in the Polish section are indicated by detectable but low concentrations of green sulfur bacteria markers. We suggest that the low concentrations of isorenieratane, paleorenieratane, and aryl isoprenoids in the studied deposits of the Appalachian Basin reflect similar environmental conditions.

Aryl isoprenoid concentrations documented in the present study are much lower than concentrations reported for Upper Devonian black shales of the Holy Cross Mountains, including those deposited in association with the Famennian Dasberg (max: 143.5 ppm TOC; Marynowski et al., 2010), Late Famennian Annulata (max: 170.2 ppm TOC; Racka et al., 2010), and the end-Famennian Hangenberg (max: 120 ppm TOC; Marynowski and Filipiak, 2007) events. While the Hangenberg event has been acknowledged as a bioevent of ecological impact nearly equivalent to that of the F/F extinction (Bambach, 2006;

Sallan and Coates, 2010), the Dasberg event is associated with the radiation of an ammonoid suborder (House, 2002). Aryl isoprenoid abundances from our Devonian sedimentary rocks are up to several orders of magnitude lower than concentrations reported from samples of oil window maturity recovered from other Phanerozoic euxinic basins (e.g., Cao et al., 2009).

The distribution of aromatic carotenoids can change with increasing thermal maturity through the oil window as C₄₀ carotenoids fragment into aryl isoprenoids, a carbon number distribution shift associated with catagenesis of all hydrocarbon compound series. Thermal cracking of the C₄₀ parent compounds into fragments is not complete until above a T_{max} of 445 °C (French et al., 2015) and the C₁₃ to C₂₂ aryl isoprenoid breakdown products (Requejo et al., 1992) remain preserved in rocks and oils at significantly higher thermal maturity compared with our black shale sample set (T_{max} of 440-444 °C). Therefore, because we quantified the aryl isoprenoid fragments together with C40 carotenoids, we best attribute the markedly lower concentrations of aryl isoprenoids of the analyzed PGB sections to rather limited, perhaps seasonal, occurrences of photic zone euxinia similar to what has been described from modern restricted basins (Tyson and Pearson, 1991). Alternatively, euxinia may have been confined to deeper waters, principally below the photic zone. Either scenario would have limited the viable habitat of green sulfur bacteria, thereby suppressing their biomass and molecular fossil abundances (Haddad et al., 2016; see also Fig. 9).

3.5. Implications for anoxia as an extinction driver

While extreme oxygen deficiency has been reported from other Late Devonian basins (Joachimski et al., 2001; Brown and Kenig, 2004; Formolo et al., 2014), our data from the northern Appalachian Basin are inconsistent with global and persistent anoxia at the F/F boundary. Indeed, results of the present study suggest that oxygen stress was not sufficiently severe and persistent to have been the controlling factor in coeval biological turnover in the Appalachian Basin. The lack of evidence of persistent anoxia or euxinia at the F/F boundary at the studied sites in New York is supported by the previous studies of Sageman et al. (2003), Boyer et al. (2014), and most recently Lash (2017). Further, variations among redox signatures described from other basins spanning the F/F cast reasonable doubt on anoxia as the primary driver of global extinction.

The cause-and-effect relationship between oxygen-poor conditions and Late Devonian bioevents has been challenged by many researchers (Stanley, 1984; Becker et al., 1991; Copper, 1998, 2002; Bratton et al., 1999; McGhee, 2001; John et al., 2010; Kazmierczak et al., 2012; George et al., 2014). Indeed, the lack of correlation between episodes of anoxia/euxinia and biodiversity crises is highlighted both in the Late Devonian and at other times in the Phanerozoic. House (2002) described at least 20 global occurrences of increased organic carbon burial during the Devonian that were not associated with extinction events, including the Frasnian Rhinestreet Shale (a massive organic-rich unit reaching about 54 m thickness along the Lake Erie shoreline in New

York State; Lash, 2016), and the Middle Devonian Marcellus Shale (which includes the Oatka Creek Formation and displays Mo values in excess of 100 ppm; Werne et al., 2002; Algeo et al., 2007). Further, some biostratigraphic extinction horizons that contain black shales in some basins appear to have accumulated in fully oxic water columns. It is noteworthy that marine invertebrate extinctions in the Late Devonian were accelerated in shallow reef settings that never experienced the highly reducing conditions documented elsewhere (e.g., most conspicuously, the Canning Basin of Western Australia, where Kellwasser facies were either not preserved or never accumulated; Becker et al., 1991; George and Chow, 2002; George et al., 2014). Rather, these extinctions involved the interaction of related factors, including climate and eustatic change, evolving paleogeography, and ocean chemistry conditions that induced a major reorganization of marine ecosystems.

Understanding the role of oxygen stress on extinction is complicated in the Late Devonian by complex signals of diversity loss driven by both extinction and failure to originate new species. However, our data are inconsistent with persistent or severe anoxia/euxinia as the primary extinction driver. The door is open, therefore, for exploration of other potential drivers, including repeated anoxic events, the combined effects of which could have accelerated extinction rates and suppressed origination rates (Boyer et al., 2014), or resulted in a collapse of speciation via habitat invasions and resource competition (Stigall, 2011). It is clear that an enhanced understanding of the role of the complex interplay of Late Devonian climate perturbations and associated eustatic variation on extinction and/or speciation loss requires detailed geochemical and paleontological investigation of strata from multiple locations.

4. Conclusions

We agree with previous work suggesting that the PGB black shales of New York State that accumulated contemporaneous with the UKw bituminous limestones of Europe record the existence of oxygen-deprived conditions at the F/F boundary. The laminated nature of these deposits, their lack of intense bioturbation and body fossils, elevated organic carbon content, high degrees of pyrite formation, trace metal proxies, and biomarkers indicative of photic zone euxinia point to restricted oxygen during deposition of the PGB. However, we find that the intensity and duration of anoxia in the Appalachian Basin at the end-Frasnian are unexceptional relative to other productive Phanerozoic marine settings. In fact, sedimentological and geochemical evidence argues in favor of baseline dysoxic bottom-water conditions occasionally interrupted by oxygenation events and episodes of photic zone euxinia. We conclude that the PGB did not accumulate under a persistently oxygen-depleted, stratified water column that experienced prolonged periods of photic zone euxinia. Instead, the UKw-equivalent black shale of the western New York State region of the Appalachian Basin was deposited under a fluctuating redox regime. Clearly, organicrich facies, some of which may be coeval with biological crises, can be deposited under a range of redox conditions, but end-member reducing environmental hotspots are not globally extensive nor representative of average global ocean chemistry conditions during these events.

Supplementary data to this article can be found online at https://doi.org/10.1016/j.palaeo.2017.10.025.

Acknowledgements

This work was funded principally by National Science Foundation Earth Sciences Program grants to GDL (NSF-EAR 1348988) and DLB (NSF-EAR 1664247). We thank Steve Bates for help with iron speciation analyses, Aaron Martinez for lab support with lipid biomarkers, Emily Seeger for help in the field, and Paul Tomascak for lab assistance. The manuscript was also improved with help from two anonymous reviewers.

References

- Algeo, T.J., 2004. Can marine anoxic events draw down the trace element inventory of seawater? Geology 32, 1057–1060.
- Algeo, T.J., Lyons, T.W., 2006. Mo-total organic carbon covariation in modern anoxic marine environments: implications for analysis of paleoredox and paleohydrographic conditions. Paleoceanography 21 (PA1016), 1–23.
- Algeo, T.J., Maynard, J.B., 2004. Trace-element behavior and redox facies in core shales of Upper Pennsylvanian Kansas-type cyclothems. Chem. Geol. 206, 289–318.
- Algeo, T.J., Berner, R.A., Maynard, J.B., Scheckler, S.E., 1995. Late Devonian oceanic anoxic events and biotic crises: "rooted" in the evolution of vascular land plants. GSA Today 5, 64–66.
- Algeo, T.J., Lyons, T.W., Blakey, R.C., Over, D.J., 2007. Hydrographic conditions of the Devono-Carboniferous North American Seaway inferred from sedimentary Mo–TOC relationships. Palaeogeogr. Palaeoclimatol. Palaeoecol. 256, 204–230.
- Algeo, T.J., Chen, Z.Q., Fraiser, M.L., Twitchett, R.J., 2011. Terrestrial-marine teleconnections in the collapse and rebuilding of Early Triassic marine ecosystems. Palaeogeogr. Palaeoclimatol. Palaeoecol. 308, 1–11.
- Allison, P.A., Wignall, P.B., Brett, C.E., 1995. Palaeo-oxygenation: effects and recognition.
 In: Bosence, D.W.J., Allison, P.A. (Eds.), Marine Palaeoenvironmental Analysis from Fossils. Geological Society Special Publication 83. pp. 97–112.
- Alroy, J., 2008a. Dynamics of origination and extinction in the marine fossil record. Proc. Natl. Acad. Sci. U. S. A. 105, 11536–11542.
- Alroy, J., 2008b. Phanerozoic trends in the global diversity of marine invertebrates. Science 321, 97–100.
- Arthur, M.A., Sageman, B.B., 1994. Marine black shales: depositional mechanisms and environments of ancient deposits. Annu. Rev. Earth Planet. Sci. 22, 499–551.
- Bambach, R.K., 2006. Phanerozoic biodiversity mass extinctions. Annu. Rev. Earth Planet. Sci. 34, 127–155.
- Bambach, R.K., Knoll, A.H., Wang, S.C., 2004. Origination, extinction, and mass depletions of marine diversity. Paleobiology 30, 522–542.
- Becker, R.T., 1993. Anoxia, eustatic changes, and Upper Devonian to lowermost Carboniferous global ammonoid diversity. In: House, M.R. (Ed.), The Ammonoidea: Environment, Ecology, and Evolutionary Change. Systematics Association Special Volume 47pp. 115–163.
- Becker, R.T., House, M.R., 1994. Kellwasser events and goniatite successions in the Devonian of the Montagne Noire with comments on possible causations. Courier-Forschung-Institut Senckenberg 16, 45–77.
- Becker, R.T., House, M.R., Kirchgasser, W.T., Playford, P.E., 1991. Sedimentary and faunal changes across the Frasnian-Famennian boundary in the canning basin of Western Australia. Hist. Biol. 5, 183–196.
- Berry, W.B.H., Wilde, P., 1978. Progressive ventilation of the oceans an explanation for the distribution of the Lower Paleozoic black shales. Am. J. Sci. 278, 257–275.
- Bond, D., Wignall, P.B., 2008. The role of sea-level change and marine anoxia in the Frasnian-Famennian (Late Devonian) mass extinction. Palaeogeogr. Palaeoclimatol. Palaeoecol. 263, 107–118.
- Bond, D., Wignall, P.B., Racki, G., 2004. Extent and duration of marine anoxia during the Frasnian–Famennian (Late Devonian) mass extinction in Poland, Germany, Austria and France. Geol. Mag. 141, 173–193.
- Boyer, D.L., Droser, M.L., 2007. Devonian monospecific assemblages: new insights into the ecology of reduced-oxygen depositional settings. Lethaia 40, 321–333.
- Boyer, D.L., Droser, M.L., 2009. Palaeoecological patterns within the dysaerobic biofacies: examples from Devonian black shales of New York state. Palaeogeogr. Palaeoclimatol. Palaeoecol. 276, 206–216.
- Boyer, D.L., Droser, M.L., 2011. A combined trace- and body- fossil approach reveals high-resolution record of oxygen fluctuations in Devonian seas. PALAIOS 26, 500–508.
- Boyer, D.L., Owens, J.D., Lyons, T.W., Droser, M.L., 2011. Joining forces: combined biological and geochemical proxies reveal a complex but refined high-resolution palaeo-oxygen history in Devonian epeiric seas. Palaeogeogr. Palaeoclimatol. Palaeoecol. 308, 134–146.
- Boyer, D.L., Haddad, E.E., Seeger, E.S., 2014. The last gasp: trace fossils track deoxygenation leading into the Frasnian-Famennian extinction event. PALAIOS 29, 646–651
- Bratton, J.F., Berry, W.B.N., Morrow, J.R., 1999. Anoxia pre-dates Frasnian–Famennian mass extinction horizon in the Great Basin, U.S.A. Palaeogeogr. Palaeoclimatol. Palaeoecol. 154, 275–292.
- Brown, T.C., Kenig, F., 2004. Water column structure during deposition of Middle Devonian-Lower Mississippian black and green/gray shales of the Illinois and Michigan Basins: a biomarker approach. Palaeogeogr. Palaeoclimatol. Palaeoecol. 215, 59–85.
- Byers, C.W., 1977. Biofacies patterns in euxinic basins: A general model. In: Cook, H.E., Enos, P. (Eds.), Deep Water Carbonate Environments. Society of Economic Paleontologists and Mineralogists, pp. 5–17.
- Calvert, S.E., Pederson, T.F., 1993. Geochemistry of Recent oxic and anoxic marine sediments: implications for the geological record. Mar. Geol. 113, 67–88.
- Canfield, D.E., Thamdrup, B., 2009. Towards a consistent classification scheme for geochemical environments, or, why we wish the term 'suboxic' would go away. Geobiology 7, 385–392.
- Canfield, D., Raiswell, R., Westrich, J., Reaves, C., Berner, R., 1986. The use of chromium reduction in the analysis of reduced inorganic sulfur in sediments and shales. Chem. Geol. 54, 149–155.
- Cao, C., Love, G.D., Hays, L.E., Bowring, S.A., Wang, W., Shen, S., Summons, R.E., 2009. Biogeochemical evidence for euxinic oceans and ecological disturbance presaging the end Permian Mass Extinction Event. Earth Planet. Sci. Lett. 281, 188–201.
- Carmichael, S.K., Waters, J.A., Suttner, T.J., Kido, E., DeReuill, A.A., 2014. A new model

- for the Kellwasser Anoxia Events (Late Devonian): shallow water anoxia in an open oceanic setting in the Central Asian Orogenic Belt. Palaeogeogr. Palaeoclimatol. Palaeoecol. 399, 394–403.
- Copper, P., 1998. Evaluating the Frasnian-Famennian mass extinction: comparing brachiopod faunas. Acta Palaeontol. Pol. 43, 137–154.
- Copper, P., 2002. Reef development at the Frasnian-Famennian mass extinction boundary. Palaeogeogr. Palaeoclimatol. Palaeoecol. 181, 27–65.
- Day, J., 1998. Distribution of latest Givetian-Frasnian Atrypida (Brachiopoda) in central and western North America. Acta Palaeontol. Pol. 43, 205–240.
- Droser, M.L., Bottjer, D.J., 1986. A semiquantitative field classification of ichnofabric. J. Sediment. Petrol. 56, 558–559.
- Droser, M.L., Bottjer, D.J., Sheehan, P.M., McGhee Jr., G.R., 2000. Decoupling of taxonomic and ecologic severity of Phanerozoic marine mass extinctions. Geology 28, 675–678.
- Duan, Y., Severmann, S., Anbar, A.D., Lyons, T.W., Gordon, G.W., Sageman, B.B., 2010. Isotopic evidence for Fe cycling and repartitioning in ancient oxygen-deficient settings: examples from black shales of the mid-to-late Devonian Appalachian basin. Earth Planet. Sci. Lett. 290, 244–253.
- Ettensohn, F.R., 1992. Controls on the origin of the Devonian-Mississippian oil and gas shales, east-central United States. Fuel 71, 1487–1492.
- Fagerstrom, J.A., 1994. The history of Devonian-Carboniferous reef communities: extinctions, effects, recovery. Facies 30, 177–192.
- Foote, M., 1994. Temporal variation in extinction risk and temporal scaling of extinction metrics. Paleobiology 20, 424–444.
- Formolo, M.J., Riedinger, N., Gill, B.C., 2014. Geochemical evidence for euxinia during the Late Devonian extinction events in the Michigan Basin (U.S.A.). Palaeogeogr. Palaeoclimatol. Palaeoecol. 414, 146–154.
- French, K.L., Rocher, D., Zumberge, J.E., Summons, R.E., 2015. Assessing the distribution of sedimentary C40 carotenoids through time. Geobiology 13, 139–151.
- Frie, A.L., Dingle, J.H., Ying, S.C., Bahreini, R., 2017. The effect of a receding saline Lake (the Salton Sea) on airborne particulate matter composition. Environ. Sci. Technol. 51, 8283–8292.
- Gallego-Torres, D., Martínez-Ruiz, F., Paytan, A., Jiménez-Espejo, F.J., Ortega-Huertas, M., 2007. Pliocene-Holocene evolution of depositional conditions in the eastern Mediterranean: role of anoxia vs. productivity at time of sapropel deposition. Palaeogeogr. Palaeoclimatol. Palaeoecol. 246, 424–439.
- George, A.D., Chow, N., 2002. The depositional record of the Frasnian/Famennian boundary interval in a fore-reef succession, Canning Basin, Western Australia. Palaeogeogr. Palaeoclimatol. Palaeoecol. 181, 347–374.
- George, A.D., Chow, N., Trinajstic, K.M., 2014. Oxic facies and the Late Devonian mass extinction, Canning Basin, Australia. Geology 42, 327–330.
- Gordon, G.W., Lyons, T.W., Arnold, G.L., Roe, J., Sageman, B.B., Anbar, A.D., 2009. When do black shales tell molybdenum isotope tales? Geology 37, 535–538. Haddad, E.E., Tuite, M.L., Martinez, A.M., Williford, K., Boyer, D.L., Droser, M.L., Love,
- Haddad, E.E., Tuite, M.L., Martinez, A.M., Williford, K., Boyer, D.L., Droser, M.L., Love, G.D., 2016. Lipid biomarker stratigraphic records through the Late Devonian Frasnian/Famennian boundary: comparison of high- and low-latitude epicontinental marine settings. Org. Geochem. 98, 38–53.
- Hallam, A., 1989. The case for sea-level change as a dominant causal factor in mass extinction of marine invertebrates. Philos. Trans. R. Soc. Lond. B325, 437–455.
- Hatch, J.R., Leventhal, J.S., 1992. Relationship between inferred redox potential of the depositional environment and geochemistry of the Upper Pennsylvanian (Missourian) stark shale member of the Dennis Limestone, Wabaunsee County, Kansas, USA. Chem. Geol. 99, 65–82.
- House, M.R., 2002. Strength, timing, setting and cause of mid-Palaeozoic extinctions. Palaeogeogr. Palaeoclimatol. Palaeoecol. 181, 5–25.
- Jablonski, D., 1991. Extinctions: a paleontological perspective. Science 253, 754–757.Joachimski, M.M., Buggisch, W., 1993. Anoxic events in the late Frasnian: causes of the Frasnian Famennian faunal crisis? Geology 21, 675–678.
- Joachimski, M.M., Ostertag-Henning, C., Pancost, R.D., Strauss, H., Freeman, K.H., Littke, R., Sinninghe Damsté, J.S., Racki, G., 2001. Water column anoxia, enhanced productivity and concomitant changes in δ¹³C and δ³⁴S across the Frasnian–Famennian boundary (Kowala Holy Cross Mountains, Poland). Chem. Geol. 175, 109–131.
- John, E.H., Wignall, P.B., Newton, R.J., Bottrell, S.H., 2010. $8^{34}S_{CAS}$ and $8^{18}O_{CAS}$ records during the Frasnian-Famennian (Late Devonian) transition and their bearing on mass extinction models. Chem. Geol. 275, 221–234.
- Johnson, J.G., Klapper, G., 1992. North American Midcontinent Devonian TR cycles. Oklahoma Geological Survey Bulletin 145, 127–135.
- Johnson, J.G., Klapper, G., Sandberg, C.A., 1985. Devonian eustatic fluctuations in Euramerica. Geol. Soc. Am. Bull. 96, 567–587.
- Jones, B., Manning, D.A.C., 1994. Comparison of geochemical indices used for the interpretation of palaeoredox conditions in ancient mudstones. Chem. Geol. 111, 111–129
- Kazmierczak, J., Kremer, B., Racki, G., 2012. Late Devonian marine anoxia challenged by benthic cyanobacterial mats. Geobiology 10, 371–383.
- Lash, G.G., 2016. Hyperpycnal transport of carbonaceous sediment example from the Upper Devonian Rhinestreet Shale, western New York, U.S.A. Palaeogeogr. Palaeoclimatol. Palaeoecol. 459, 29–43.
- Lash, G.G., 2017. A multiproxy analysis of the Frasnain-Famennian transition in western New York State, U.S.A. Palaeogeogr. Palaeoclimatol. Palaeoecol. 473, 108–122.
- Levin, L.A., 2003. Oxygen minimum zone benthos: adaptation and community response to hypoxia. Oceanogr. Mar. Biol. Annu. Rev. 41, 1–45.
- Levman, B.G., Von Bitter, P.H., 2002. The Frasnian–Famennian (mid-Late Devonian) boundary in the type section of the Long Rapids Formation, James Bay Lowlands, northern Ontario, Canada. Can. J. Earth Sci. 39, 1795–1818.
- Lüning, S., Adamson, K., Craig, J., 2003. Frasnian organic-rich shales in North Africa: regional distribution and depositional model. In: Arthur, T.J., MacGregor, D.S.,

- Cameron, N.R. (Eds.), Petroleum Geology of Africa: New Themes and Developing Technologies. Geological Society of London Special Publications 207pp. 165–184.
- Lyons, T.W., Severmann, S., 2006. A critical look at iron paleoredox proxies: new insights from modern euxinic marine basins. Geochim. Cosmochim. Acta 70, 5698–5722.
- Lyons, T.W., Berner, R.A., Anderson, R.F., 1993. Evidence for large pre-industrial perturbations of the Black Sea chemocline. Nature 365, 538–540.
- Lyons, T.W., Werne, J.P., Hollander, D.J., Murray, R.W., 2003. Contrasting sulfur geochemistry and Fe/Al and Mo/Al ratios across the last oxic-to-anoxic transition in the Cariaco Basin, Venezuela. Chem. Geol. 195, 131–157.
- Lyons, T.W., Anbar, A.D., Severmann, S., Scott, C., Gill, B.C., 2009. Tracking euxinia in the ancient ocean: a multiproxy perspective and Proterozoic case study. Annu. Rev. Earth Planet. Sci. 37, 507–534.
- Marynowski, L., Filipiak, P., 2007. Water column euxinia and wildfire evidence during deposition of the Upper Famennian Hangenberg event horizon from the Holy Cross Mountains (central Poland). Geol. Mag. 144, 569–595.
- Marynowski, L., Rakociński, M., Zatoń, M., 2007. Middle Famennian (Late Devonian) interval with pyritized fauna from the Holy Cross Mountains (Poland): organic geochemistry and pyrite framboid diameter study. Geochem. J. 41, 187–200.
- Marynowski, L., Filipiak, P., Zatoń, M., 2010. Geochemical and palynological study of the Upper Famennian Dasberg event horizon from the Holy Cross Mountains (central Poland). Geol. Mag. 147, 527–550.
- Marynowski, L., Rakociński, M., Borcuch, E., Kremer, B., Schubert, B.A., Jahren, A.H., 2011. Molecular and petrographic indicators of redox conditions and bacterial communities after the F/F mass extinction (Kowala, Holy Cross Mountains, Poland). Palaeogeogr. Palaeoclimatol. Palaeoecol. 306, 1–14.
- Marynowski, L., Zatoń, M., Rakociński, M., Filipiak, P., Kurkiewicz, S., Pearce, T.J., 2012. Deciphering the upper Famennian Hangenberg Black Shale depositional environments based on multi-proxy record. Palaeogeogr. Palaeoclimatol. Palaeoecol. 346-347, 66-86.
- Maslen, E., Grice, K., Gale, J.D., Hallmann, C., Horsfield, B., 2009. Crocetane: a potential marker of photic zone euxinia in thermally mature sediments and crude oils of Devonian age. Org. Geochem. 40, 1–11.
- McGhee Jr., G.R., 1996. The Late Devonian Mass Extinction: The Frasnian-Famennian Crisis. Columbia University Press, New York.
- McGhee Jr., G.R., 2001. The 'multiple impacts hypothesis' for mass extinction: a comparison of the Late Devonian and the late Eocene. Palaeogeogr. Palaeoclimatol. Palaeoecol. 176, 47–58.
- McGhee Jr., G.R., Sheehan, P.M., Bottjer, D.J., Droser, M.L., 2004. Ecological ranking of Phanerozoic biodiversity crises: ecological and taxonomic severities are decoupled. Palaeogeogr. Palaeoclimatol. Palaeoecol. 211, 289–297.
- McManus, J., Berelson, W.M., Klinkhammer, G.P., Hammond, D.E., Holm, C., 2005. Authigenic uranium: relationship to oxygen penetration depth and organic carbon rain. Geochim. Cosmochim. Acta 69, 95–108.
- McManus, J., Berelson, W.M., Severmann, S., Poulson, R.L., Hammond, D.E., Klinkhammer, G.P., Holm, C., 2006. Molybdenum and uranium geoochemistry in continental margin sediments: paleoproxy potential. Geochim. Cosmochim. Acta 70, 4643–4662.
- Melendez, I., Grice, K., Trinajstic, K., Ladjavardi, M., Greenwood, P., Thompson, K., 2012. Biomarkers reveal the role of photic zone euxinia in exceptional fossil preservation: an organic geochemical perspective. Geology 41, 123–126.
- Melendez, I., Grice, K., Schwark, L., 2013. Exceptional preservation of Palaeozoic steroids in a diagenetic continuum. Sci Rep 3, 2768.
- Morford, J.L., Emerson, S., 1999. The geochemistry of redox sensitive trace metals in sediments. Geochim. Cosmochim. Acta 63, 1735–1750.
- Morford, J.L., Russell, A.D., Emerson, S., 2001. Trace metal evidence for changes in the redox environment associated with the transition from terrigenous clay to diatomaceous sediments, Saanich Inlet, BC. Mar. Geol. 174, 355–369.
- Murphy, A.E., Sageman, B.B., Hollander, D.J., Lyons, T.W., Brett, C.E., 2000a. Black shale deposition and faunal overturn in the Devonian Appalachian basin: clastic starvation, seasonal water-column mixing, and efficient biolimiting nutrient recycling. Paleoceanography 15, 280–291.
- Murphy, A.E., Sageman, B.B., Hollander, D.J., 2000b. Eutrophication by decoupling of the marine biogeochemical cycles of C, N, and P: a mechanism for the Late Devonian mass extinction. Geology 28, 427–430.
- Over, D.J., 1997. Conodont biostratigraphy of the Java Formation (Upper Devonian) and the Frasnian–Famennian boundary in western New York State. Geol. Soc. Am. Spec. Pap. 321, 161–177.
- Over, D.J., 2002. The Frasnian–Famennian boundary in central and eastern United States. Palaeogeogr. Palaeoclimatol. Palaeoecol. 181, 153–169.
- Over, D.J., Baird, G.C., Kirchgasser, W.T., 2013. Middle-Upper Devonian strata along the Lake Erie Shore, Western New York. In: New York State Geological Association Field Trip Guidebook, 85th Annual Meeting, pp. 182–219.
- Ozalas, K., Savrda, C.E., Fullerton, R., 1994. Bioturbated oxygenation-event beds in siliceous facies: Monterey Formation (Miocene), California. Palaeogeogr. Palaeoclimatol. Palaeoecol. 112, 63–83.
- Pattan, J.N., Pearce, N.J.G., 2009. Bottom water oxygenation history in southeastern Arabian Sea during the past 140 ka: results from redox-sensitive elements. Palaeogeogr. Palaeoclimatol. Palaeoecol. 280, 396–405.
- Poulton, S.W., Canfield, D.E., 2005. Development of a sequential extraction procedure for iron: implications for iron partitioning in continentally derived particulates. Chem. Geol. 214, 209–221.
- Poulton, S.W., Canfield, D.E., 2011. Ferruginous conditions: a dominant feature of the ocean through earth's history. Elements 7, 107–112.
- Quinby-Hunt, M.S., Wilde, P., 1994. Thermodynamic zonation in the black shale facies based on iron-manganese-vanadium content. Chem. Geol. 113, 297–317.
- Racka, M., Marynowski, L., Filipiak, P., Sobstel, M., Pisarzowska, A., Bond, D.P.G., 2010.

- Anoxic annulata events in the late Famennian of the Holy Cross Mountains (Southern Poland): geochemical and palaeontological record. Palaeogeogr. Palaeoclimatol. Palaeoecol. 297, 549–575.
- Racki, G., Racka, M., Matyja, H., Devleeschouwer, X., 2002. The Frasnian/Famennian boundary interval in the South Polish-Moravian shelf basins: integrated event-stratigraphical approach. Palaeogeogr. Palaeoclimatol. Palaeoecol. 181, 251–297.
- Raiswell, R., Canfield, D.E., 1998. Sources of iron for pyrite formation in marine sediments. Am. J. Sci. 298, 219–245.
- Raiswell, R., Newton, R., Wignall, P.B., 2001. An indicator of water-column anoxia: resolution of biofacies variations in the Kimmeridge Clay (Upper Jurassic, U.K.). J. Sediment. Res. 71, 286–294.
- Raup, D.M., Sepkoski Jr., J.J., 1982. Mass extinctions in the marine fossil record. Science 215, 1501–1503.
- Reinhard, C.T., Lyons, T.W., Rouxel, O., Asael, D., Dauphas, N., Kump, L.R., 2012. Iron speciation and isotope perspective on Palaeoproterozoic water column chemistry. In: Melezhik, V.A., Kump, L.R., Strauss, H., Prave, A.R. (Eds.), Reading the Archive of Earth's Oxygenation: Volume 3: Global Events and the Fennoscandian Arctic Russia-Drilling Early Earth Project, pp. 1483–1492.
- Reinhard, C.T., Planavsky, N.J., Robbins, L.J., Partin, C.A., Gill, B.C., Lalonde, S.V., Bekker, A., Konhauser, K.O., Lyons, T.W., 2013. Proterozoic ocean redox and biogeochemical stasis. Proc. Natl. Acad. Sci. 110, 5357–5362.
- Requejo, A.G., Allan, J., Creaney, S., Gray, N.R., Cole, K.S., 1992. Aryl isoprenoids and diaromatic carotenoids in Paleozoic source rocks and oils from Western Canada and Williston Basins. Org. Geochem. 19, 245–264.
- Rhoads, D.C., Morse, J.W., 1971. Evolutionary and ecologic significance of oxygen-deficient marine basins. Lethaia 4, 413–428.
- Rimmer, S.M., 2004. Geochemical paleoredox indicators in Devonian-Mississippian black shales, Central Appalachian Basin (USA). Chem. Geol. 206, 373–391.
- Sageman, B.B., Murphy, A.E., Werne, J.P., ver Straeten, C.A., Hollander, D.J., Lyons, T.W., 2003. A tale of shales: the relative roles of production, decomposition, and dilution in the accumulation of organic-rich strata, Middle-Upper Devonian, Appalachian Basin. Chem. Geol. 195, 229–273.
- Sallan, L.C., Coates, M.I., 2010. End-Devonian extinction and a bottleneck in the early evolution of modern jawed vertebrates. Proc. Natl. Acad. Sci. U. S. A. 107, 10131–10135.
- Savrda, C.E., 1992. Trace fossils and benthic oxygenation. In: Maples, C.G., West, R.R. (Eds.), Trace Fossils: Short Courses in the Paleontological Society, pp. 172–196.
- Savrda, C.E., Bottjer, D.J., 1986. Trace fossil model for reconstruction of paleo-oxygenation in bottom waters. Geology 14, 3–6.
- Savrda, C.E., Bottjer, D.J., 1989. Trace fossil model for reconstructing oxygenation histories of ancient marine bottom-waters: application to Upper Cretaceous Niobrara Formation, Colorado. Palaeogeogr. Palaeoclimatol. Palaeoecol. 74, 49–74.
- Schwark, L., Empt, P., 2006. Sterane biomarkers as indicators of Palaeozoic algal evolution. Palaeogeogr. Palaeoclimatol. Palaeoecol. 240, 225–236.
- Scott, C., Lyons, T.W., 2012. Contrasting molybdenum cycling and isotopic properties in euxinic versus non-euxinic sediments and sedimentary rocks: refining the paleoproxies. Chem. Geol. 324–325, 19–27.
- Scott, C., Lyons, T.W., Bekker, A., Shen, Y., Poulton, S.W., Chu, X., Anbar, A.D., 2008. Tracing the stepwise oxygenation of the Proterozoic ocean. Nature 452, 456–459.
- Shanmugam, G., Spalding, T.D., Rofheart, D.H., 1993. Traction structures in deep-marine bottom-current reworked sands in the Pliocene and Pleistocene, Gulf of Mexico. Geology 21, 929–932.
- Sperling, E.A., Halverson, G.P., Knoll, A.H., Macdonald, F.A., Johnston, D.T., 2013. A

- basin redox transect at the dawn of animal life. Earth Planet. Sci. Lett. 371-372, 143-155.
- Sperling, E.A., Frieder, C.A., Levin, L.A., 2016. Biodiversity response to natural gradients of multiple stressors on continental margins. Proc. R. Soc. B 283, 20160637.
- Stachacz, M., Uchman, A., Rodríguez-Tovar, F.J., 2017. Ichnological record of the Frasnian-Famennian boundary interval: two examples from the Holy Cross Mts (Central Poland). Int. J. Earth Sci. 106, 157–170.
- Stanley, S.M., 1984. Temperature and biotic crises in the marine realm. Geology 12, 205–208.
- Stigall, A.L., 2011. Speciation collapse and invasive species dynamics during the Late Devonian "Mass Extinction". GSA Today 22, 4–9.
- Summons, R.E., Powell, T.G., 1986. Chlorobiaceae in Palaeozoic seas—combined evidence from biological markers, isotopes and geology. Nature 319, 763–765.
- Thompson, J.B., Mullins, H.T., Newton, C.R., Vercoutere, T.L., 1985. Alternative biofacies model for dysaerobic communities. Lethaia 18, 167–179.
- Tribovillard, N., Averbuch, O., Devleeschouwer, X., Racki, G., Riboulleau, A., 2004. Deepwater anoxia over the Frasnian-Famennian boundary (La Serre, France): a tectonically induced oceanic anoxic event? Terra Nova 16, 288–295.
- Tribovillard, N., Algeo, T.J., Lyons, T., Riboulleau, A., 2006. Trace metals as paleoredox and paleoproductivity proxies: an update. Chem. Geol. 232, 12–32.
- Tyson, R.V., Pearson, T.H., 1991. Modern and ancient continental shelf anoxia: an overview. In: Tyson, R.V., Pearson, T.H. (Eds.), Modern and Ancient Continental Shelf Anoxia. Geological Society Special Publication 58pp. 1–24.
- Wedepohl, K.H., 1971. Environmental influences on the chemical composition of shales and clays. In: Ahrens, L.H., Press, F., Runcorn, S.K., Urey, H.C. (Eds.), Physics and Chemistry of the Earth. vol. 8. Pergamon, Oxford, pp. 305–333.
- Wedepohl, K.H., 1991. The composition of the upper earth's crust and the natural cycles of selected metals. Metals in natural raw materials. Natural resources. In: Merian, E. (Ed.), Metals and Their Compounds in the Environment. VCH, Weinheim, pp. 3–17.
- Wedepohl, K.H., 1995. The composition of the continental crust. Geochim. Cosmochim. Acta 50, 1217–1232.
- Werne, J.P., Sageman, B.B., Lyons, T.W., Hollander, D.J., 2002. An integrated assessment of a "type euxinic" deposit: evidence for multiple controls on black shale deposition in the Middle Devonian Oatka Creek Formation. Am. J. Sci. 302, 110–143.
- Wetzel, A., Uchmann, A., 1998. Biogenic sedimentary structures in mudstones an overview. In: Schieber, J., Zimmerle, W., Sethi, P. (Eds.), Shales and Mudstones I. E. Schweizerbart'sche Verlagsbuchhandlung (Nägele u. Obermiller), Stuttgart, pp. 351–360
- Wignall, P.B., 1994. Black shales. In: Oxford Monographs on Geology and Geophysics, 30.
 Oxford Science Publications. Oxford.
- Wilde, P., Berry, W.B.N., 1984. Destabilization of the oceanic density structure and its significance to marine "extinction" events. Palaeogeogr. Palaeoclimatol. Palaeoecol. 48, 143–162
- Wilde, P., Berry, W.B.N., 1986. The role of oceanographic factors in the generation of global bio-events. In: Walliser, O.H. (Ed.), Global Bio-events. Lecture Notes in Earth Sciences, vol. 9. Springer-Verlag, Berlin, pp. 75–91.
- Wilson, R.D., Schieber, J., 2015. Sedimentary facies and depositional environment of the Middle Devonian Geneseo Formation of New York, U.S.A. J. Sediment. Res. 85, 1393–1415.
- Woulds, C., Cowie, G.L., Levin, L.A., Andersson, J.H., Middelburg, J.J., Vandewiele, S., Lamont, P.A., Larkin, K.E., Gooday, A.J., Schumacher, S., Whitcraft, C., Jeffreys, R.M., Schwartz, M., 2007. Oxygen as a control on seafloor biological communities and their roles in sedimentary carbon cycling. Limnol. Oceanogr. 52, 1698–1709.